Supporting Information

A Bioinspired Approach to Reversibly Metal Binding Interfaces

Agnes C. Morrissey,[#] Vishakya Jayalatharachchi,[#] Lukas Michalek, Prasanna Egodawatta, Neomy Zaquen, Laura Delafresnaye,* Christopher Barner-Kowollik*

A. C. Morrissey, Dr. V. Jayalatharachchi, Dr. L. Michalek, Dr. L. Delafresnaye, Prof. Dr. C. Barner-Kowollik
School of Chemistry and Physics
Queensland University of Technology (QUT)
2 George Street, 4000 Brisbane, Queensland, Australia
E-mail: christopher.barnerkowollik@qut.edu.au; laura.delafresnaye@qut.edu.au

A/Prof P. Egodawatta
School of Civil and Environmental Engineering
Queensland University of Technology (QUT)
2 George Street, 4000 Brisbane, Queensland, Australia

Prof. Dr. C. Barner-Kowollik
Institute of Nanotechnology (INT),
Hermann-von-Helmholtz-Platz 1
Karlsruhe Institute of Technology (KIT),
76344 Eggenstein-Leopoldshafen, Germany

Dr. N. Zaquen
Lapinus, ROCKWOOL B.V.
Delfstoffenweg 2, 6045JH Roermond, The Netherlands

[#]These authors have contributed equally.

Contents

1 Materials

All chemicals and solvents were used as received from the supplier without further purification, unless stated otherwise.

Acetonitrile (Chemsupply), tetrahydrofuran (Thermo Fisher), ethyl acetate (Thermo Fisher), dichloromethane (Chemsupply), methanol (Thermo Fisher), dimethyl sulfoxide (Thermo Fisher), ethanol (Thermo Fisher), water (Milli-Q, Merck), 3,4-Dihydroxy-L-phenylalanine (Sigma-Aldrich), *tert*-butyldimethylsilyl chloride (95%, Sigma-Aldrich), 1,8-diazabicyclo[5.4.0]undec-7-ene (99%, Sigma-Aldrich), sodium bicarbonate (Sigma-Aldrich), di-*tert*-butyl dicarbonate (Sigma-Aldrich), hydrochloric acid (32% solution, Thermo Fisher), magnesium sulfate (Merck), N-Ethyl-N′-(3-dimethylaminopropyl)carbodiimide (98%, Thermo Fisher), 11-bromo-1-undecanol (Thermo Fisher), 4-Dimethylaminopyridine (Merck), sodium chloride (Thermo Fisher), tetra-*n*-butylammonium fluoride in tetrahydrofuran (1.0 M) (Sigma-Aldrich), acetic acid (glacial, Thermo Fisher), potassium hydroxide (Thermo Fisher), 1,6-hexanediol (99%, Sigma-Aldrich), 4′-chloro-2,2′:6′,2″-terpyridine (99%, Sigma-Aldrich), tris(hydroxymethyl)aminomethane (Merck), ethylenediaminetetraacetic acid (Thermo Fisher), zinc trifluoromethanesulfonate (98%, Sigma-Aldrich), nickel(II) chloride (98%, Sigma-Aldrich), Sodium hydroxide (Thermo Fisher).

Methanol-d_4 (99.8%, Sigma-Aldrich), chloroform-d_1 ($CDCl_3$, 99.8%, Sigma-Aldrich), and dimethyl sulfoxide-d_6 (DMSO-d_6 , 99.9%, Sigma-Aldrich) were utilized as solvent for NMR measurements.

2 Instrumentation

Flash chromatography: Flash column chromatography was performed on an Interchim XS420+ flash chromatography system consisting of a SP-in-line filter 20-µm, an UV/Vis detector (200-800 nm) and a SofTA Model 400 ELSD (55 °C dift tube temperature, 25 °C spray chamber temperature, filter 5, EDR gain mode) connected via a flow splitter (Interchim Split ELSD F04590). The separations were performed using an Interchim dry load column (dryload on celite 565) and an Interchim Puriflash Silica HP 30 µm column.

Nuclear Magnetic Resonance (NMR) Spectrometry: ^{1}H- and ^{13}C NMR-spectra were recorded on a Bruker System 600 Ascend LH, equipped with a BBO-Probe (5 mm) with z-gradient (^{1}H 600.13 MHz, ^{13}C 150.90 MHz) at 298 K. Resonances are reported in parts per million (ppm) relative to tetramethylsilane (TMS).

UV-visible Spectroscopy: UV/Vis spectra were recorded on a Shimadzu UV-2700 spectrophotometer equipped with a CPS-100 electronic temperature control cell positioner. Samples were prepared in chloroform and measured in Hellma Analytics quartz high precision cells with a path length of 10 mm at 20 °C. The spectra were recorded in a range of 250 to 700 nm.

Liquid chromatography–mass spectrometry (LCMS): LC-MS measurements were performed on an UltiMate 3000 UHPLC System (Dionex, Sunnyvale, CA, USA) consisting of a pump (LPG 3400SZ), autosampler (WPS 3000TSL) and a temperature-controlled column compartment (TCC 3000). Separation was performed on a C18 HPLC column (Phenomenex Luna 5µm, 100 Å, 250 × 2.0 mm) operating at 40 °C. Water (containing 5 mmol L^{-1} ammonium acetate) and acetonitrile were used as eluents. A gradient of acetonitrile: H_2O, 5:95 to 100:0 (v/v) in 7 min at a flow rate of 0.40 mL·min^{-1} was applied. The flow was split in a 9:1 ratio, where 90% of the eluent was directed through a DAD UV-detector (VWD 3400, Dionex) and 10% was infused into the electrospray source. Spectra were recorded on an LTQ Orbitrap Elite mass spectrometer (Thermo Fisher Scientific, San Jose, CA, USA) equipped with a HESI II probe. The instrument was calibrated in the m/z range 74-1822 using premixed calibration solutions (Thermo Scientific). A constant spray voltage of 3.5 kV, a dimensionless sheath gas, and a dimensionless auxiliary gas flow rate of 5 and 2 were applied, respectively. The capillary

temperature was set to 300 °C, the S-lens RF level was set to 68, and the aux gas heater temperature was set to 100 °C.

X-ray photoelectron spectroscopy (XPS): XPS spectra were collected using a Kratos Axis Supra system operating with a monochromatic Al Kα source (1486.7 eV). Survey spectra and high-resolution core-level spectra were collected with pass energies of 160 and 20 eV respectively and a step size of 0.1 eV. All XPS data were processed with CasaXPS. All spectra were calibrated by setting the C 1s peak to 285.00 eV.

Time of Flight- Secondary Ion Mass Spectroscopy (ToF-SIMS): Data were acquired using an IONTOF M6 ToF-SIMS instrument (IONTOF GmbH, Germany) with a reflectron time-of-flight analyser and 30 keV Bi/Mn primary-ion source. Bi^{3+} cluster ions were selected from the pulsed primary-ion beam for the analysis and "bunched" for optimal mass resolution. Surface charging was compensated by flooding the sample with low-energy (20 eV) electrons between primary-ion pulses. The pressure in the analysis chamber was at below 1×10^{-9} mbar. Data were acquired in both positive and negative polarities, and the mass scales were calibrated using spectral peaks attributed to either C^+, CH^+, $CH^{2+,}$ and CH^{3+}, or C^-, CH^{2-}, $C^{3-,}$ and C^{4-}, respectively. Recalibration to positive-ion data was achieved using peaks covering a similar mass range to that used in negative polarity. All data were processed with the built-in module of the SurfaceLab 7.2 software (IONTOF GmbH).

Atomic Force Microscopy (AFM): A Bruker Icon PT atomic force microscope was used in PeakForce Tapping mode with a scanAsyst-air probe to study the thickness of the coating on Si surface. All images were processed using Nanoscope Analysis 2.0.

Scanning Electron Microscopy (SEM): SEM images were captured using Tescan MIRA3 using an in-lens SE detector at an 8 mm working distance using a 5 kV acceleration voltage. Samples were prepared by dispersing Fibres onto a conductive carbon tape. Samples were coated with a 3 nm platinum layer.

3 Synthesis

3.1 2-amino-3-(3,4-bis((*tert*-butyldimethylsilyl)oxy)phenyl)propanoic acid (1)

The synthesis of compound **1** and **2** was adapted from a literature procedure.[1]

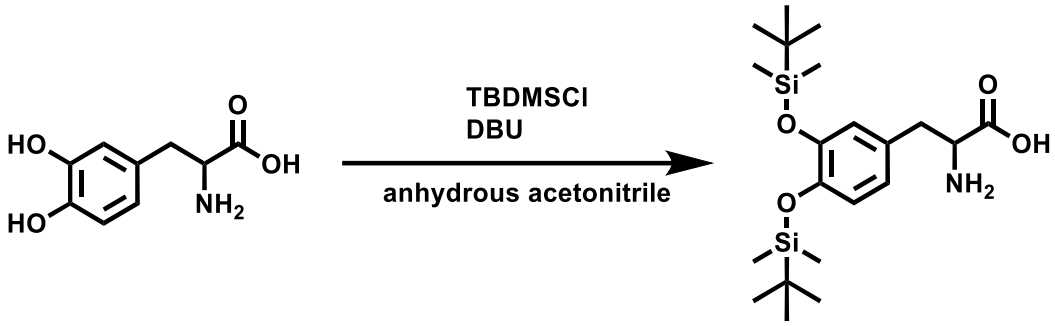

3,4-Dihydroxy-L-phenylalanine (1.60 g, 8.0 mmol) and *tert*-butyldimethylsilyl chloride (3.60 g, 24.0 mmol) were dissolved in 18 mL dry acetonitrile. The reaction mixture was cooled to 0 °C. Subsequently, 1,8-diazabicyclo[5.4.0]undec-7-ene (3.6 mL, 24.0 mmol) was added dropwise and the reaction mixture was stirred at ambient temperature for 24 h. The addition of cold acetonitrile (20 mL) resulted in the precipitation of a white solid. The precipitate was filtered and dried under vacuum.

Yield: 1.80 g (53%)

^{1}H NMR (600 MHz, d_4 - MeOD): δ = 0.22 (d, 12H, Si-CH_3), 1.00 (d, 18H, C(CH_3), 2.84 (m, 1H, CH_2), 3.20 (m, 1H, CH_2), 3.67 (m, 1H, C*H*), 6.75 – 6.85 (3H, *H*-aromatic) ppm.

^{13}C NMR (150 MHz, d_4 - MeOD): δ = -3.5, 19.6, 26.8, 37.9, 58.0, 122.7, 123.7, 130.9, 148.2, 174.1 ppm.

LC-MS: calculated: m/z = 426.2490 $[M+H]^+$; found: m/z = 426.2494 $[M+H]^+$.

3.2 3-(3,4-bis((*tert*-butyldimethylsilyl)oxy)phenyl)-2-((*tert*-butoxycarbonyl)amino) propanoic acid (2)

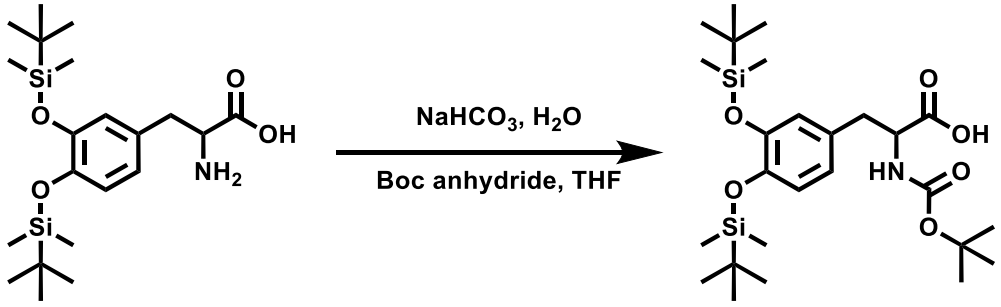

Sodium bicarbonate (0.32 g, 3.77 mmol) and 2-amino-3-(3,4-bis((*tert*-butyldimethylsilyl)oxy)phenyl)propanoic acid (1.5 g, 3.52 mmol) were dissolved in 20 mL water. Di-*tert*-butyl dicarbonate (0.87 g, 4.00 mmol) dissolved in 20 mL tetrahydrofuran was added and the reaction mixture was stirred for 24 h at ambient temperature. tetrahydrofuran was evaporated and 10 mL of water was added to the residue. The solution was acidified with dilute HCl to pH 5. The aqueous phase was extracted with ethyl acetate (3 x 30 mL). The combined organic phases were dried over magnesium sulphate and the solvent was evaporated.

Yield: 1.55 g (58%)

^{1}H NMR (600 MHz, d_4 - MeOD): δ = 0.19 (d, 12H, Si-CH_3), 0.99 (d, 18H, C(CH_3), 1.39 (s, 9H, O-C(CH_3)$_3$), 2.78 (m, 1H, CH_2), 3.03 (m, 1H, CH_2), 4.24 (m, 1H, C*H*), 6.69 – 6.76 (3H, *H*-aromatic) ppm.

^{13}C NMR (150 MHz, d_4 - MeOD): δ = -4.1, 19.0, 26.4, 28.5, 38.0, 56.7, 80.1, 121.7, 123.1, 132.1, 146.5, 147.4, 157.4, 171.3 ppm.

LC-MS: calculated: m/z = 524.2858 $[M-H]^-$; found: m/z = 524.2863 $[M-H]^-$.

3.3 11-bromoundecyl 3-(3,4-bis((*tert*-butyldimethylsilyl)oxy)phenyl)-2-((*tert*-butoxycarbonyl)amino)propanoate (3)

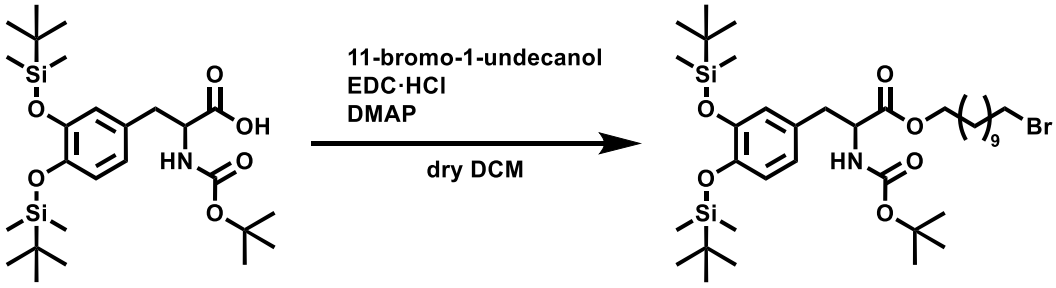

EDC·HCl (1.97 g, 10.30 mmol) and 3-(3,4-bis((*tert*-butyldimethylsilyl)oxy)phenyl)-2-((*tert*-butoxycarbonyl)amino) propanoic acid (1.80 g, 3.42 mmol) were dissolved in 100 mL dry dichloromethane and the reaction mixture was stirred for 30 min at ambient temperature. Next, 11-bromo-1-undecanol (1.04 g, 4.12 mmol) and DMAP (0.42 g, 3.45 mmol) were added to the reaction mixture and the reaction mixture was stirred for 20 h at ambient temperature. 50 mL dichloromethane was added to the reaction mixture and the organic phase was extracted with brine (4 x 50 mL) and water (4 x 50 mL).

The organic phase was dried over magnesium sulphate and purified *via* column chromatography (dichloromethane : methanol = 1 : 0.1)

Yield: 0.99 g (38%)

^{1}H NMR (600 MHz, $CDCl_3$): δ = 0.18 (d, 12H, Si-CH_3), 0.98 (d, 18H, C(CH_3), 1.27 (m, 14H, CH_2), 1.42 (s, 9H, O-C(CH_3)$_3$), 1.59 (m, 2H, CH_2), 1.85 (m, 2H CH_2), 2.95 (m, 2H, CH_2), 3.40 (t, 2H, CH_2), 4.07 (m, 2H, CH_2), 4.50 (m, 1H, CH), 6.55 – 6.72 (3H, *H*-aromatic) ppm.

^{13}C NMR (150 MHz, $CDCl_3$): δ = -4.1, 18.4, 25.8-29.6, 32.8, 34.0, 37.5, 54.3. 65.4, 79.7, 120.9, 128.9, 146.6, 171.9, 188.0 ppm.

LC-MS: calculated: m/z = 780.3661 $[M+Na]^+$; found: m/z = 780.3652 $[M+Na]^+$.

3.4 11-bromoundecyl 2-((*tert*-butoxycarbonyl)amino)-3-(3,4-dihydroxyphenyl)propanoate (4)

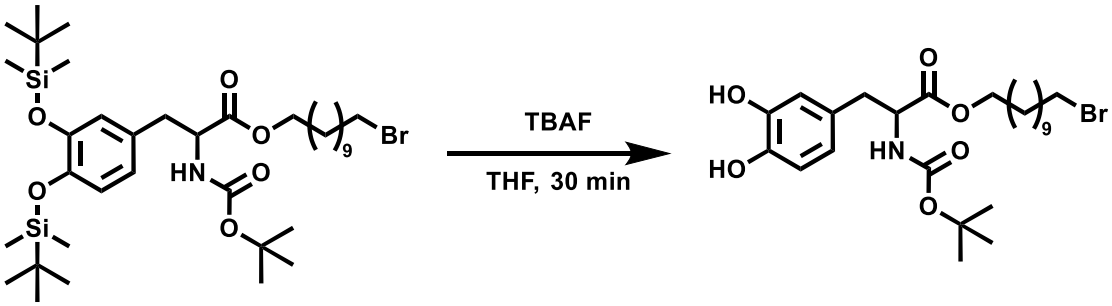

11-bromoundecyl 3-(3,4-bis((*tert*-butyldimethylsilyl)oxy)phenyl)-2-((*tert*-butoxycarbonyl) amino)propanoate (0.25 g, 0.33 mmol) was dissolved in 1 mL tetrahydrofuran. Tetra-*n*-butylammonium fluoride (TBAF) (0.65 mL, 0.65 mmol) in THF (1.0 M) was added and the reaction mixture was stirred for 30 min at ambient temperature. The solvent was evaporated, and the residue was dissolved in dichloromethane. The organic phase was extracted with water (2 x 15 mL), diluted Hac (0.05 M) (2 x 15 mL), brine (2 x 15 mL) and water (2 x 15 mL). The organic phase was dried over magnesium sulphate and the solvent was removed. The product was applied for the surface reactions immediately.

Yield: 0.12 g (71%)

LC-MS: calculated: m/z = 552.1931 $[M+Na]^+$; found: m/z = 552.1930 $[M+Na]^+$.

3.5 **6-([2,2':6',2''-terpyridin]-4'-yloxy)hexan-1-ol (5)**

The synthesis of compound **5** was adapted from a literature procedure.[2]

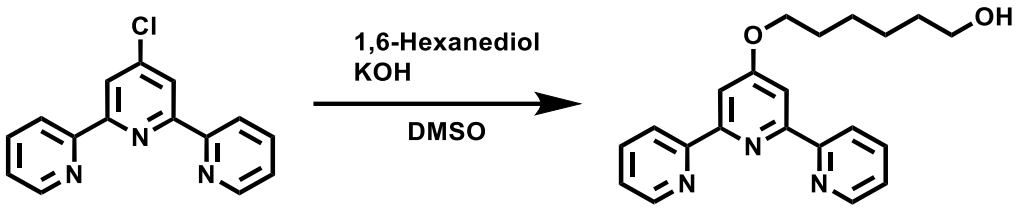

Potassium hydroxide (0.51 g, 9.15 mmol) was suspended in 13 mL DMSO and stirred at 40 °C for 15 min. Subsequently, 1,6-hexanediol (2.22 g, 18.79 mmol) was added and stirred for 30 min at 40 °C. Subsequently, 4′-chloro-2,2′:6′,2″-terpyridine (0.50 g, 1.87 mmol) was added and stirred at 40 °C for 4 h. The reaction mixture was poured into water (300 mL) and after 15 h the white precipitate was filtered off and washed three times with water. After drying at 40 °C under vacuum a colourless solid was obtained.

Yield: 0.28 g (43%)

^{1}H NMR (600 MHz, $CDCl_3$): δ = 1.43 – 1.84 (m, 8H,CH_2), 3.61 (m, 2H, -CH_2-OH), 4.27 (m, 2H, -CH_2-O-), 7.38 (m, 2H, *H*-Tpy5,5´´), 7.91 (m, *H*-Tpy4, 4´´), 8.08 (s, 2H, *H*-Tpy3´,5´), 8.64 (m, 2H, *H*-Tpy6,6´´), 8.70 (m, 2H, *H*-Tpy3,3´´) ppm.

^{13}C NMR (150 MHz, $CDCl_3$): δ = 25.4, 25.7, 28.9, 32.6, 62.8, 68.0, 107.4, 121.3, 123.7, 136.8, 149.0, 156.1, 157.0, 167.3 ppm.

LC-MS: calculated: m/z = 350.1861 $[M+H]^+$; found: m/z = 350.1863 $[M+H]^+$.

3.6 6-([2,2':6',2''-terpyridin]-4'-yloxy)hexyl 3-(3,4-bis((*tert*-butyldimethylsilyl)oxy) phenyl)-2-((*tert*-butoxycarbonyl)amino)propanoate (6)

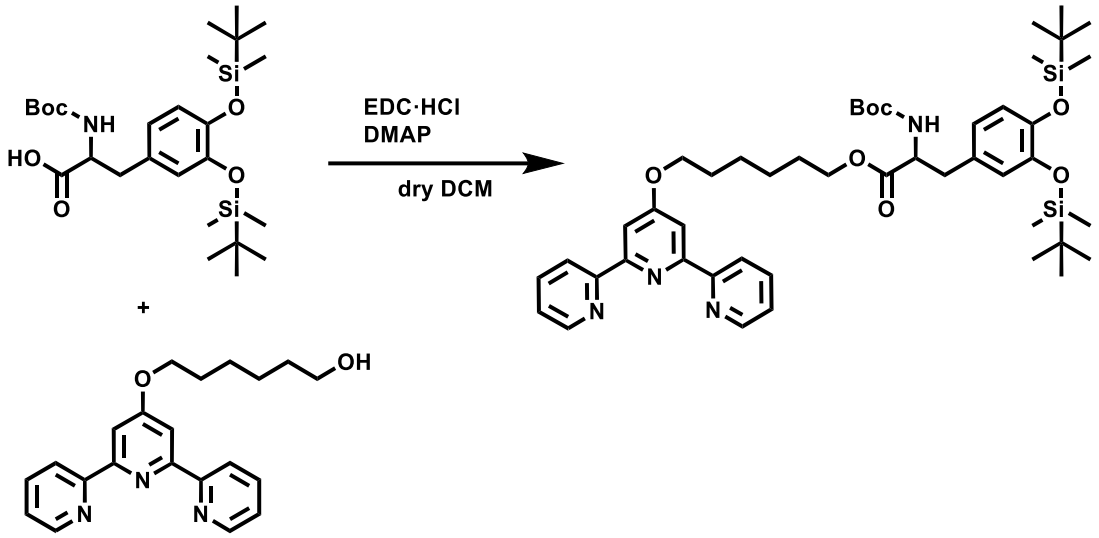

EDC·HCl (0.83 g, 4.30 mmol) and 6-([2,2':6',2"-terpyridin]-4'-yloxy)hexan-1-ol (0.50 g, 1.43 mmol) were dissolved in 100 mL dry dichloromethane and the reaction mixture was stirred for 30 min at ambient temperature. 3-(3,4-bis((*tert*-butyldimethylsilyl)oxy)phenyl)-2-((*tert*-butoxycarbonyl)amino)propanoic acid (1.00 g, 1.90 mmol) and DMAP (0.18 g, 1.43 mmol) were added to the reaction mixture. The reaction mixture was stirred for 20 h at ambient temperature. 20 mL dichloromethane was added, and the organic phase was extracted with brine (4 x 50 mL) and water (4 x 50 mL). The organic phase was dried over magnesium sulphate and purified *via* column chromatography (dichloromethane: methanol = 1 : 0.1).

Yield: 1.027 g (84%)

^{1}H NMR (600 MHz, $CDCl_3$): δ = 0.18 (m, 12H, Si-C*H*$_3$), 0.97 (m, 18H, C(C*H*$_3$), 1.39 (s, 9H, O-C(C*H*$_3$)$_3$), 1.45 (m, 2H, C*H*$_2$), 1.54 (m, 2H, C*H*$_2$), 1.66 (m, 2H, C*H*$_2$), 1.87 (m, 2H, C*H*$_2$), 2.95 (m, 2H, C*H*$_2$ (DOPA)), 4.10-4.28 (m, 4H, -C*H*$_2$-O-, -C*H*$_2$-OH), 4.50 (m, 1H, C*H*), 6.55 – 6.73 (3H, *H*-aromatic), 7.39 (m, 2H, *H*-Tpy5,5´´), 7.92 (m, *H*-Tpy4, 4´´), 8.09 (s, 2H, *H*-Tpy3´,5´), 8.67 (m, 2H, *H*-Tpy6,6´´), 8.73 (m, 2H, *H*-Tpy3,3´´) ppm.

^{13}C NMR (150 MHz, $CDCl_3$): δ = -4.2, 18.4, 25.6, 25.7, 25.9, 28.3, 28.4, 28.9, 37.4, 54.3, 65.2, 67.9, 79.7, 107.3, 120.9, 121.3, 122.2, 123.7, 128.9, 136.7, 145.8, 146.6, 149.0, 155.0, 156.1, 157.0, 167.2, 171.9 ppm.

LC-MS: calculated: m/z = 857.4699 $[M+H]^+$; found: m/z = 857.4681 $[M+H]^+$.

3.7 6-([2,2':6',2''-terpyridin]-4'-yloxy)hexyl 2-((*tert*-butoxycarbonyl)amino)-3-(3,4-dihydroxyphenyl)propanoate (7)

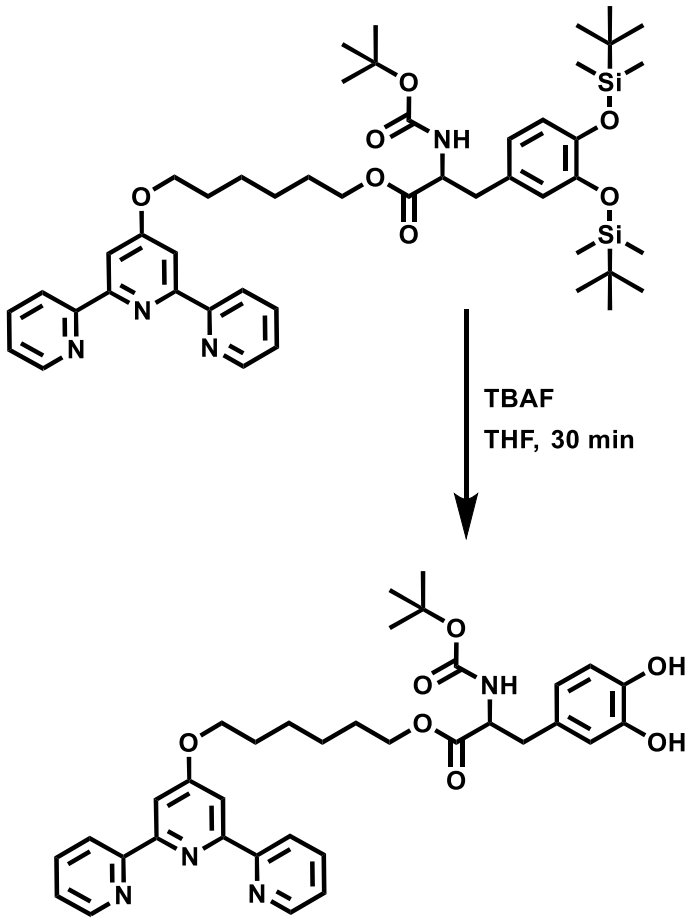

6-([2,2':6',2''-terpyridin]-4'-yloxy)hexyl 3-(3,4-bis((*tert*-butyldimethylsilyl)oxy)phenyl)-2-((*tert*-butoxycarbonyl)amino)propanoate (0.28 g, 0.33 mmol) was dissolved in 1 mL tetrahydrofuran. Tetra-*n*-butylammonium fluoride (TBAF) (0.65 mL, 0.65 mmol) in THF (1.0 M) was added and the reaction mixture was stirred for 30 min at room temperature. The solvent was evaporated, and the residue was dissolved in dichloromethane. The organic phase was extracted with water (2 x 15 mL), diluted Hac (0.05 M) (2 x 15 mL), brine (2 x 15 mL) and water (2 x 15 mL). The organic phase was dried over magnesium sulphate and the solvent was removed. The product was applied for the surface reactions immediately.

Yield: 0.18 g (88%)

^{1}H NMR (600 MHz, DMSO): δ = 1.33 (s, 9H, O-C(C*H*$_3$)$_3$), 1.36 (m, 2H, C*H*$_2$), 1.47 (m, 2H, C*H*$_2$), 1.55 (m, 2H, C*H*$_2$), 1.80 (m, 2H, C*H*$_2$), 2.73 (m, 2H, C*H*$_2$ (DOPA)), 4.02 (m, 3H, -C*H*$_2$-O-, C*H*), 4.26 (m, 2H, -C*H*$_2$-O-), 6.45 (m, 1H, *H*-aromatic), 6.60 (m, 2H, *H*-aromatic), 7.16 (m, 1H, N*H*), 7.54 (m, 2H, *H*-Tpy5,5´´), 8.00 (s, *H*-Tpy4, 4´´), 8.05 (m, 2H, *H*-Tpy3´,5´), 8.64 (m, 2H, *H*-Tpy6,6´´), 8.73 (m, 2H, *H*-Tpy3,3´´) ppm.

^{13}C NMR (150 MHz, DMSO): δ = 25.3, 28.3, 28.6, 36.3, 56.1, 64.5, 68.3, 78.5, 107.4, 115.6, 116.7, 120.0, 121.4, 125.0, 128.5, 138.2, 144.1, 145.2, 149.2, 154.6, 156.4, 167.2 ppm.

LC-MS: calculated: m/z = 629.2970 $[M+H]^+$; found: m/z = 629.2967 $[M+H]^+$.

4 NMR spectra

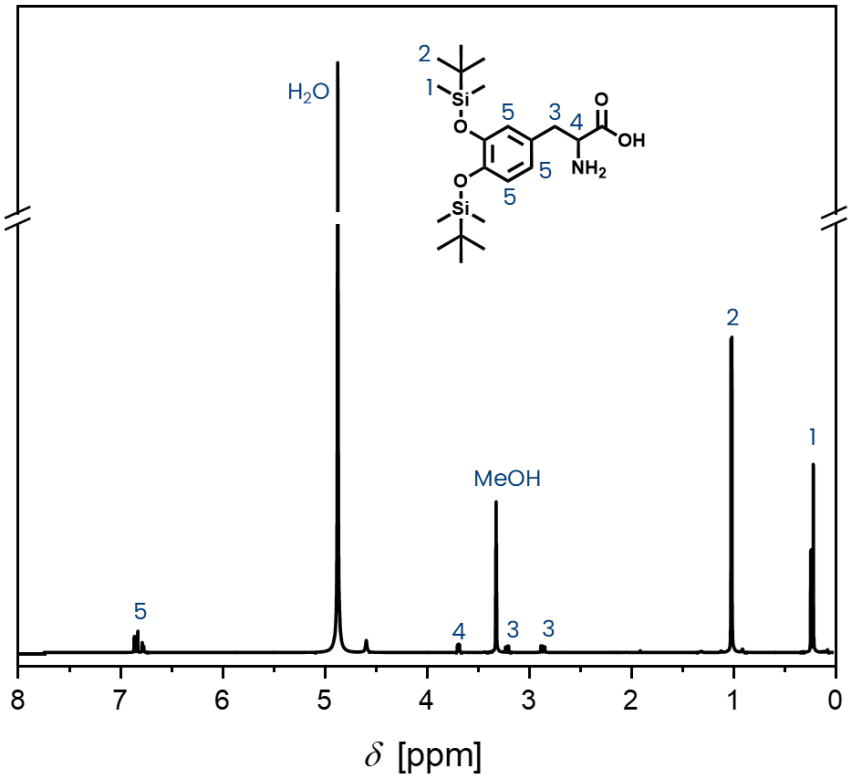

Figure S1. ^{1}H NMR spectrum of 2-amino-3-(3,4-bis((*tert*-butyldimethylsilyl)oxy)phenyl) propanoic acid (MeOD, 600 MHz).

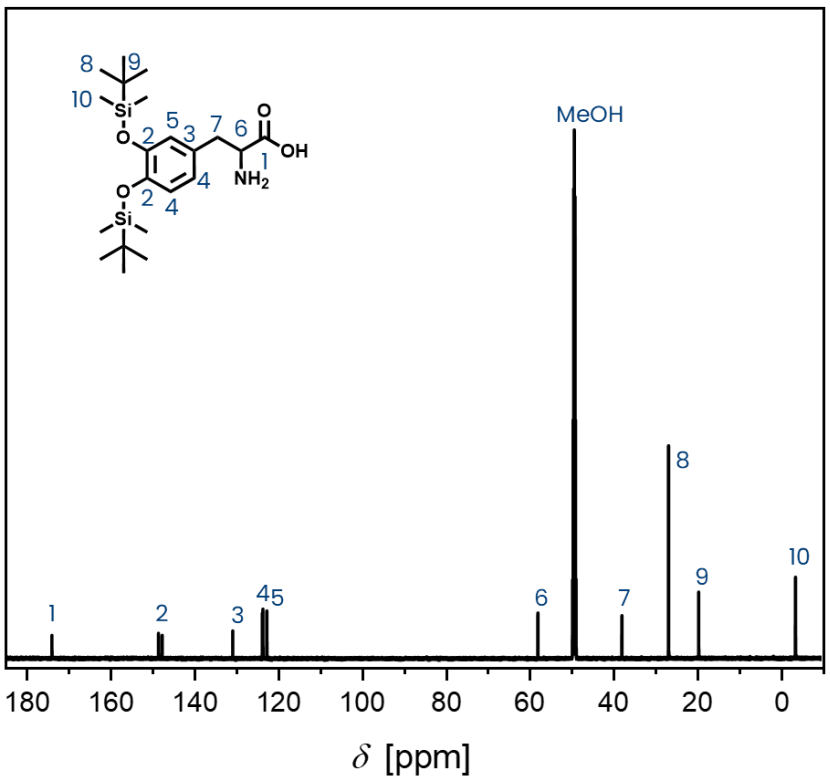

Figure S2 ^{13}C NMR spectrum of 2-amino-3-(3,4-bis((*tert*-butyldimethylsilyl)oxy)phenyl) propanoic acid (MeOD, 150 MHz).

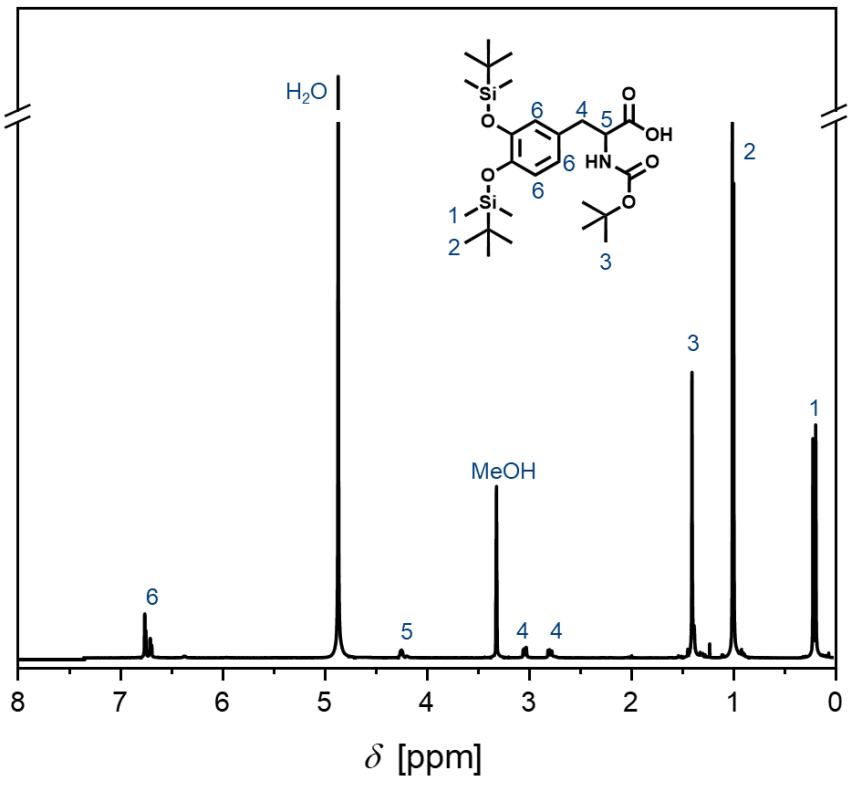

Figure S3. ^{1}H NMR spectrum of 3-(3,4-bis((*tert*-butyldimethylsilyl)oxy)phenyl)-2-((*tert*-butoxycarbonyl)amino) propanoic acid (MeOD, 600 MHz).

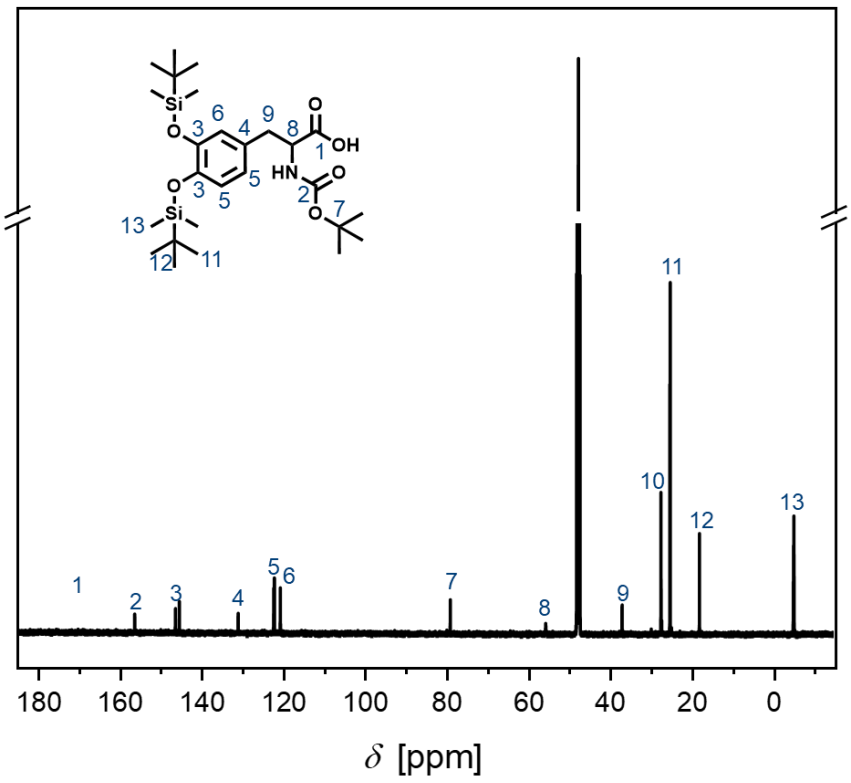

Figure S4. ^{13}C NMR spectrum of 3-(3,4-bis((*tert*-butyldimethylsilyl)oxy)phenyl)-2-((*tert*-butoxycarbonyl)amino) propanoic acid (MeOD, 150 MHz).

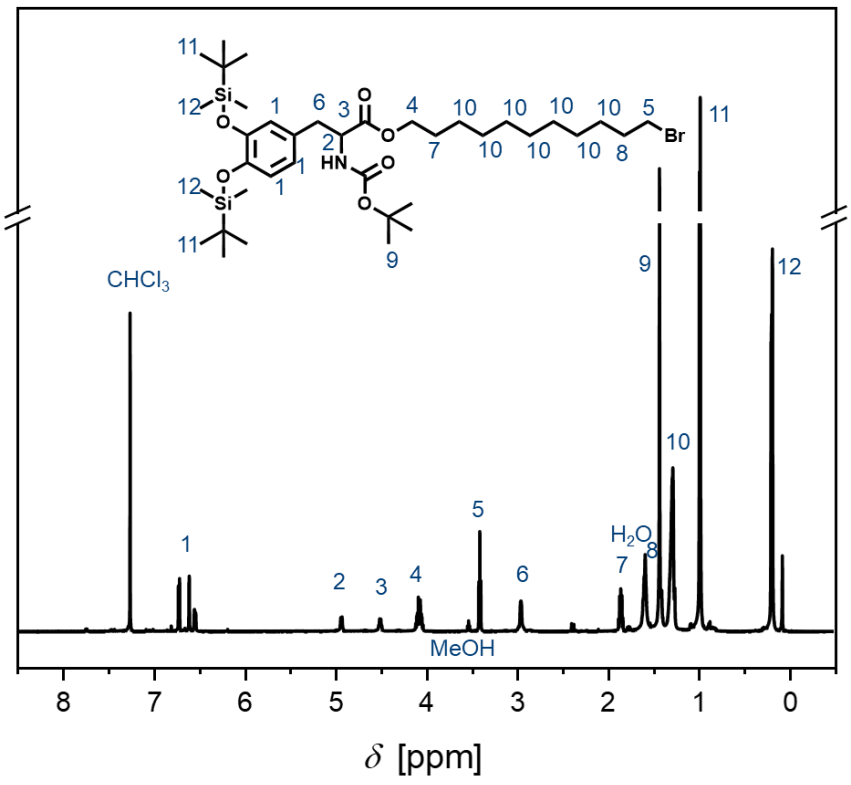

Figure S5. ^{1}H NMR spectrum of 11-bromoundecyl 3-(3,4-bis((*tert*-butyldimethylsilyl)oxy)phenyl)-2-((*tert*-butoxycarbonyl)amino)propanoate ($CDCl_3$, 600 MHz).

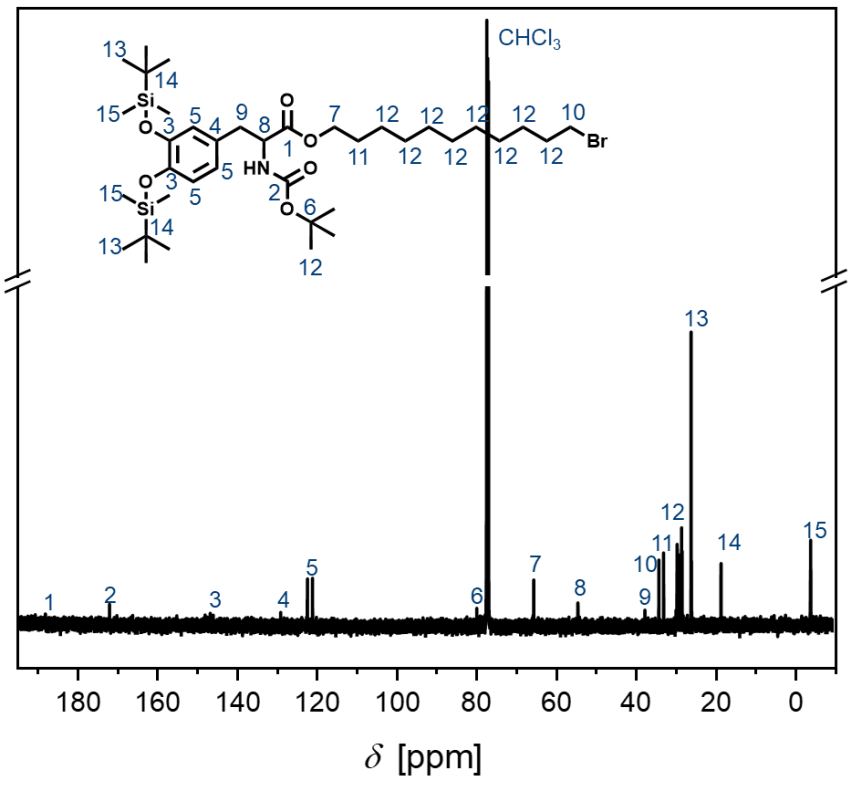

Figure S6. ^{13}C NMR spectrum of 11-bromoundecyl 3-(3,4-bis((*tert*-butyl dimethylsilyl)oxy)phenyl)-2-((*tert*-butoxycarbonyl)amino)propanoate ($CDCl_3$, 150 MHz).

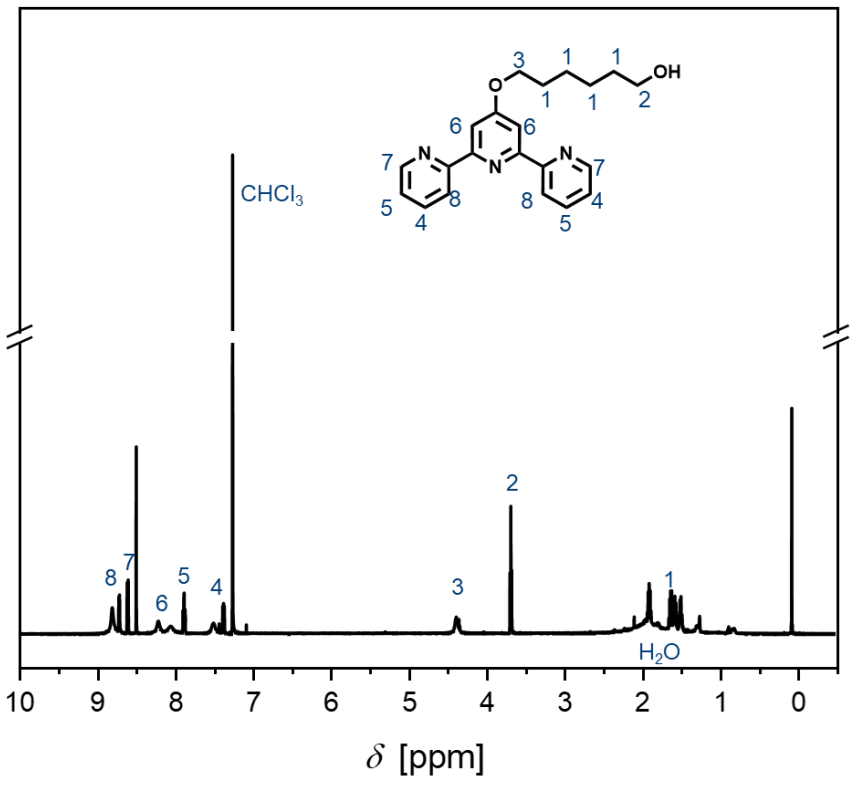

Figure S7. ^{1}H NMR spectrum of 6-([2,2':6',2"-terpyridin]-4'-yloxy)hexan-1-ol ($CDCl_3$, 600 MHz).

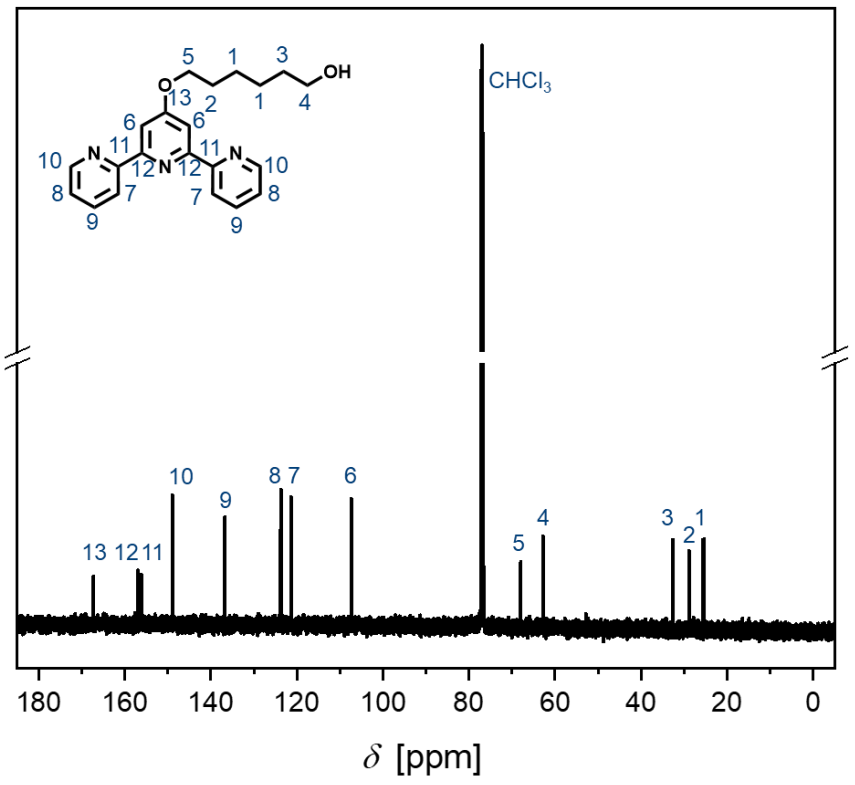

Figure S8. ^{13}C NMR spectrum of 6-([2,2':6',2"-terpyridin]-4'-yloxy)hexan-1-ol ($CDCl_3$, 150 MHz).

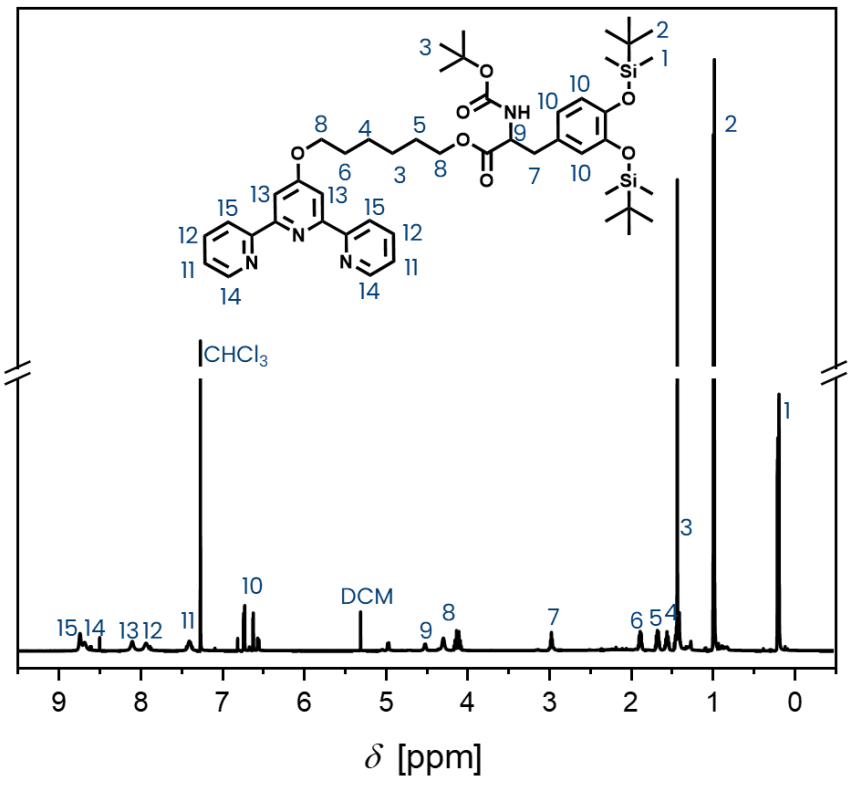

Figure S9. ^{1}H NMR spectrum of 6-([2,2':6',2"-terpyridin]-4'-yloxy)hexyl 3-(3,4-bis((*tert*-butyldimethylsilyl)oxy)phenyl)-2-((*tert*-butoxycarbonyl)amino)propanoate ($CDCl_3$, 600 MHz).

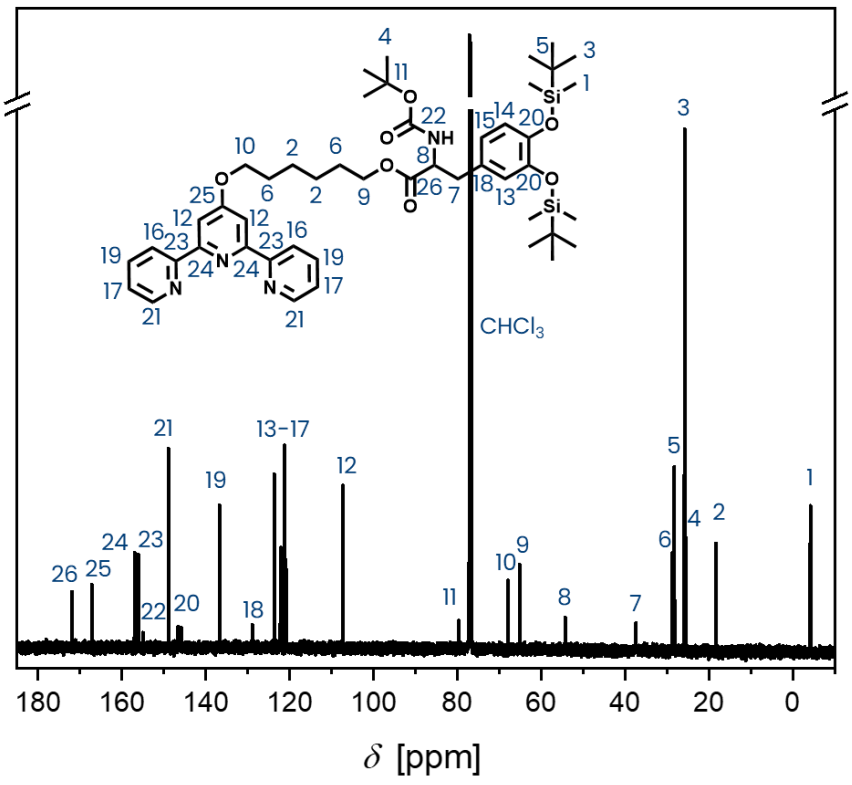

Figure S10. ^{13}C NMR spectrum of 6-([2,2':6',2''-terpyridin]-4'-yloxy)hexyl 3-(3,4-bis((*tert*-butyldimethylsilyl)oxy)phenyl)-2-((*tert*-butoxycarbonyl)amino)propanoate ($CDCl_3$, 150 MHz).

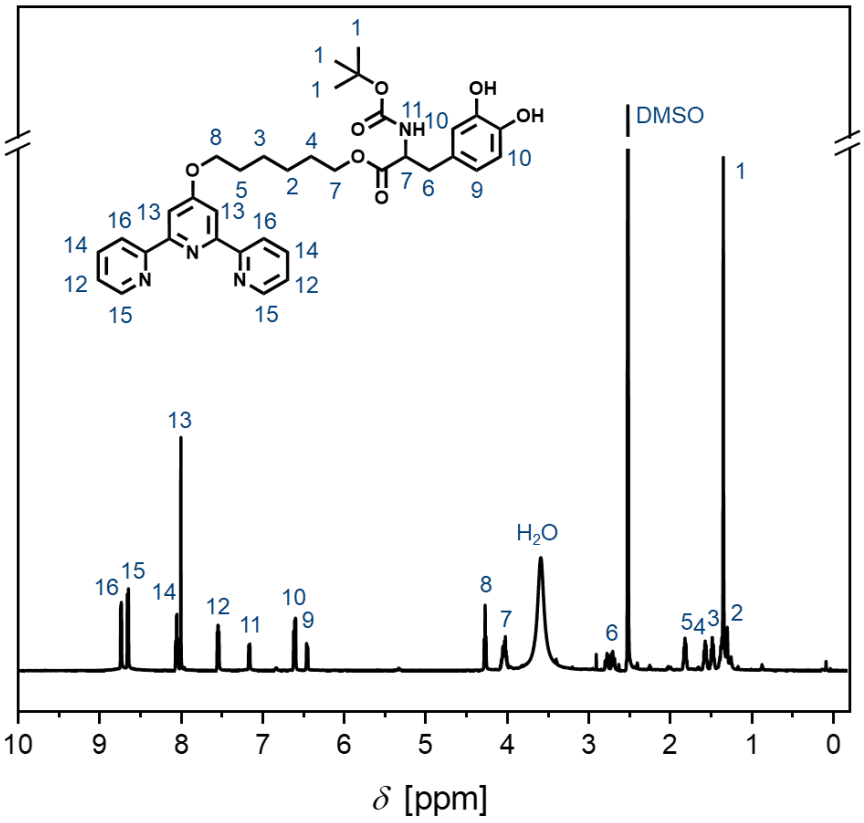

Figure S11. ^{1}H NMR spectrum of 6-([2,2':6',2"-terpyridin]-4'-yloxy)hexyl 2-((*tert*-butoxy carbonyl)amino)-3-(3,4-dihydroxyphenyl)propanoate (DMSO, 600 MHz).

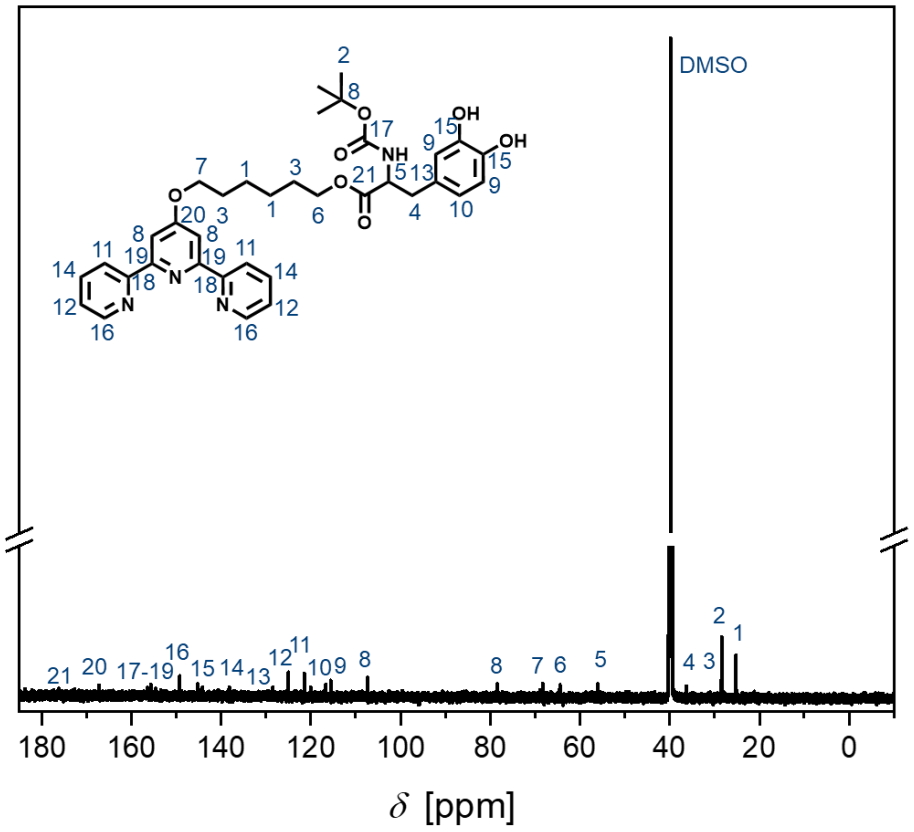

Figure S12. ^{13}C NMR spectrum of 6-([2,2':6',2"-terpyridin]-4'-yloxy)hexyl 2-((*tert*-butoxy carbonyl)amino)-3-(3,4-dihydroxyphenyl)propanoate (DMSO, 150 MHz).

5 Mass spectrometry

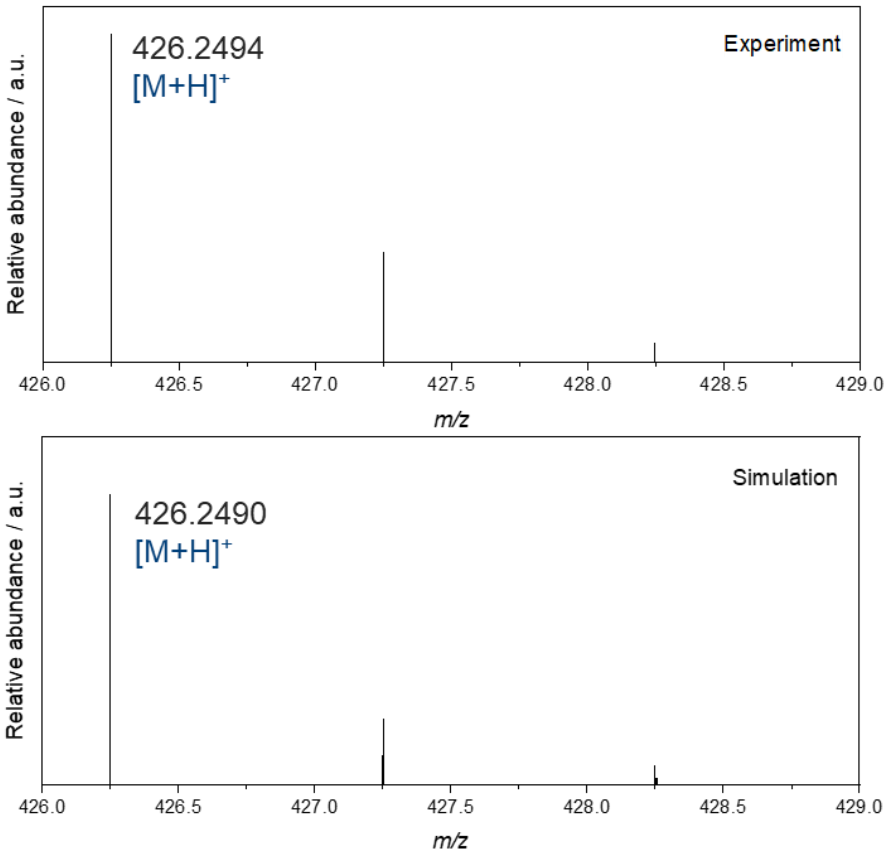

Figure S13. Experimental (top) and simulated (bottom) mass spectrum of compound **1**.

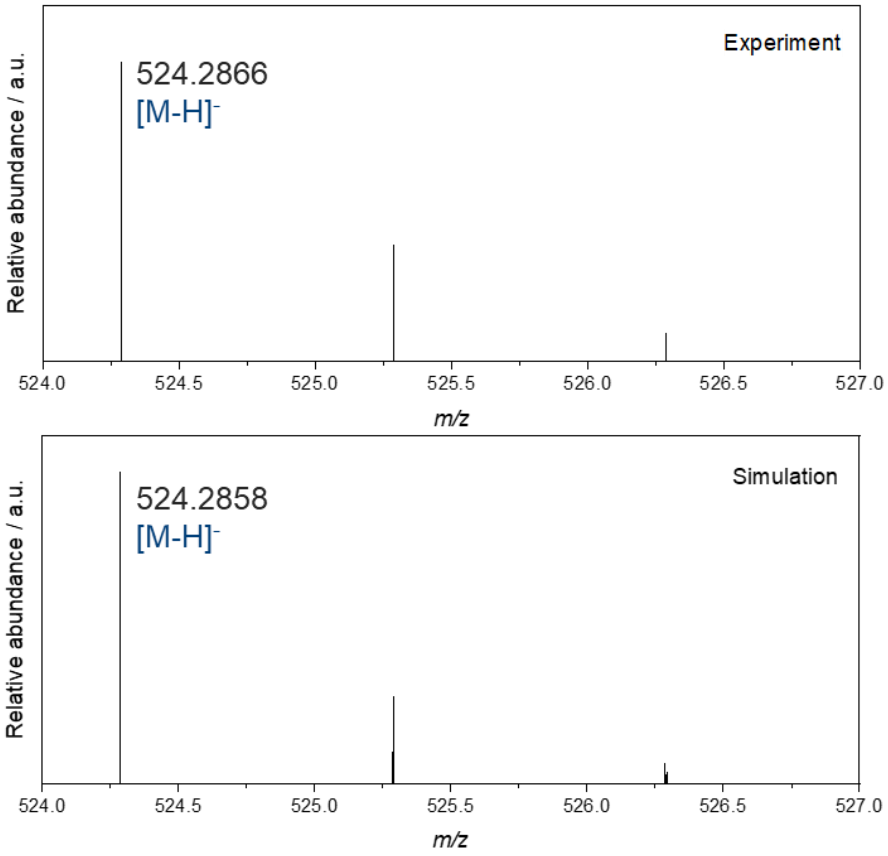

Figure S14. Experimental (top) and simulated (bottom) mass spectrum of compound **2**.

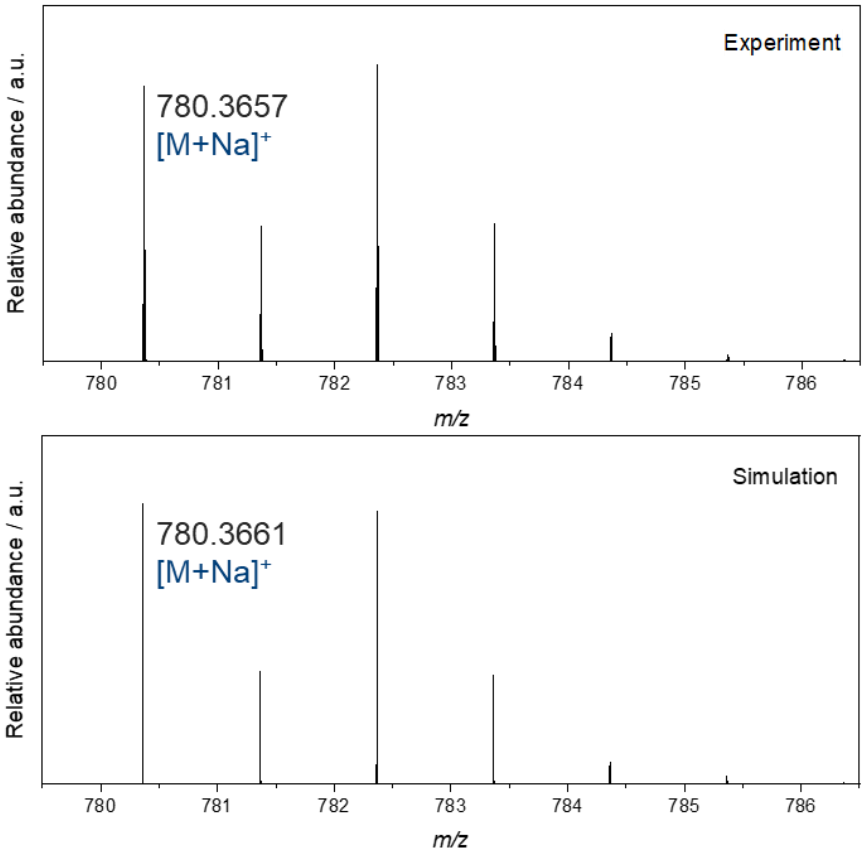

Figure S15. Experimental (top) and simulated (bottom) mass spectrum of compound **3**.

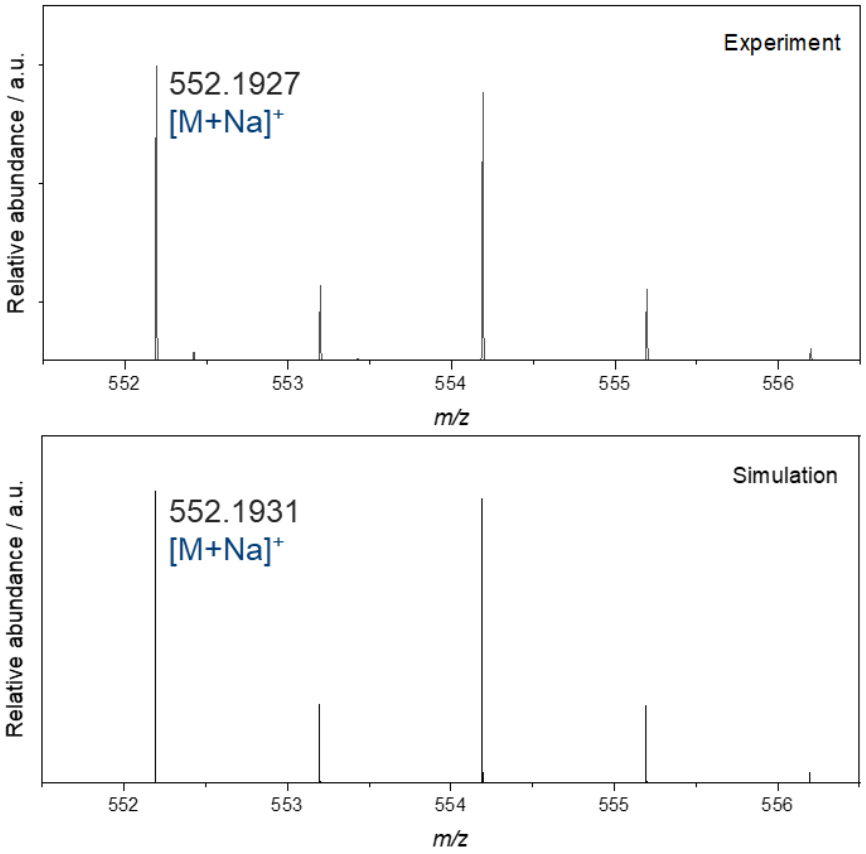

Figure S16. Experimental (top) and simulated (bottom) mass spectrum of compound **4**.

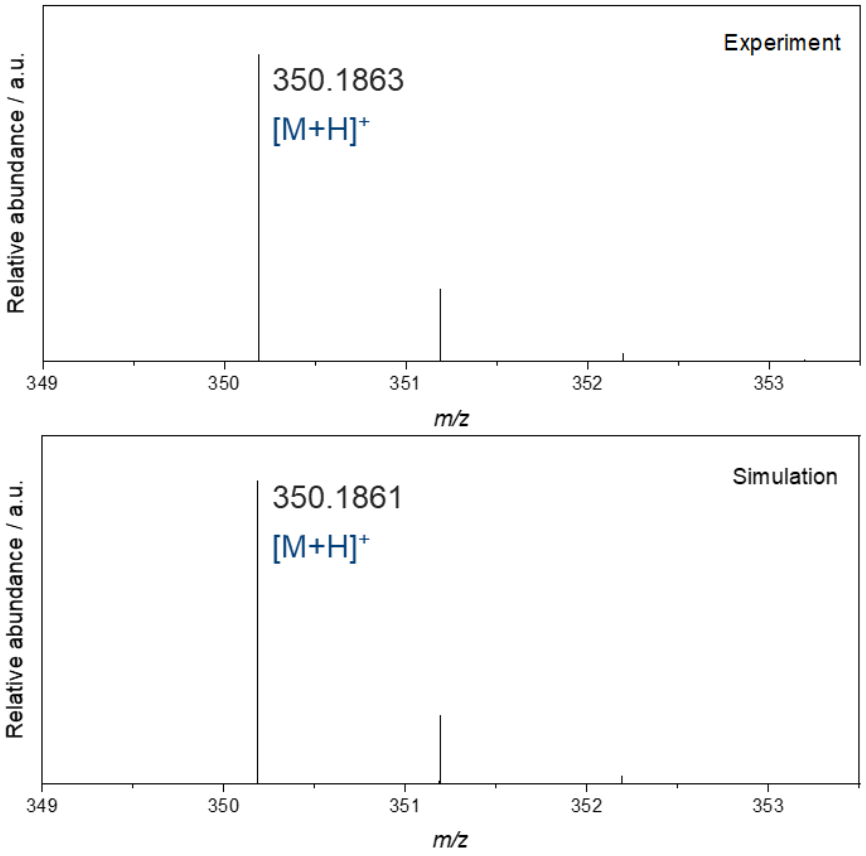

Figure S17. Experimental (top) and simulated (bottom) mass spectrum of compound **5**.

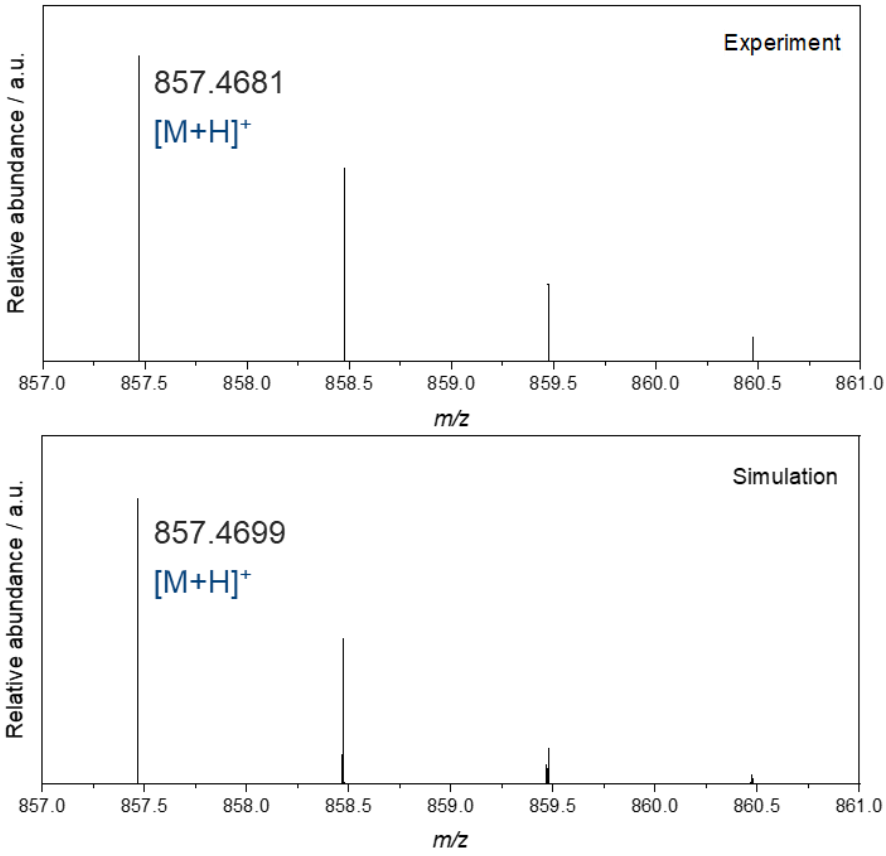

Figure S18. Experimental (top) and simulated (bottom) mass spectrum of compound **6**.

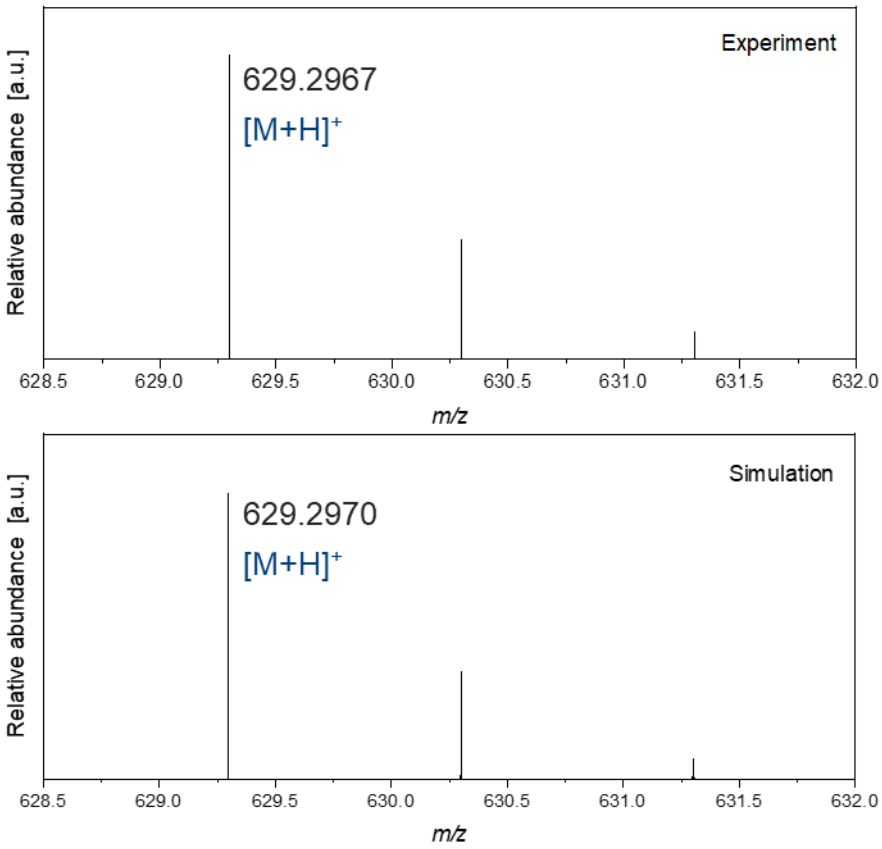

Figure S19. Experimental (top) and simulated (bottom) mass spectrum of compound **7**.

6 UV/Vis measurements

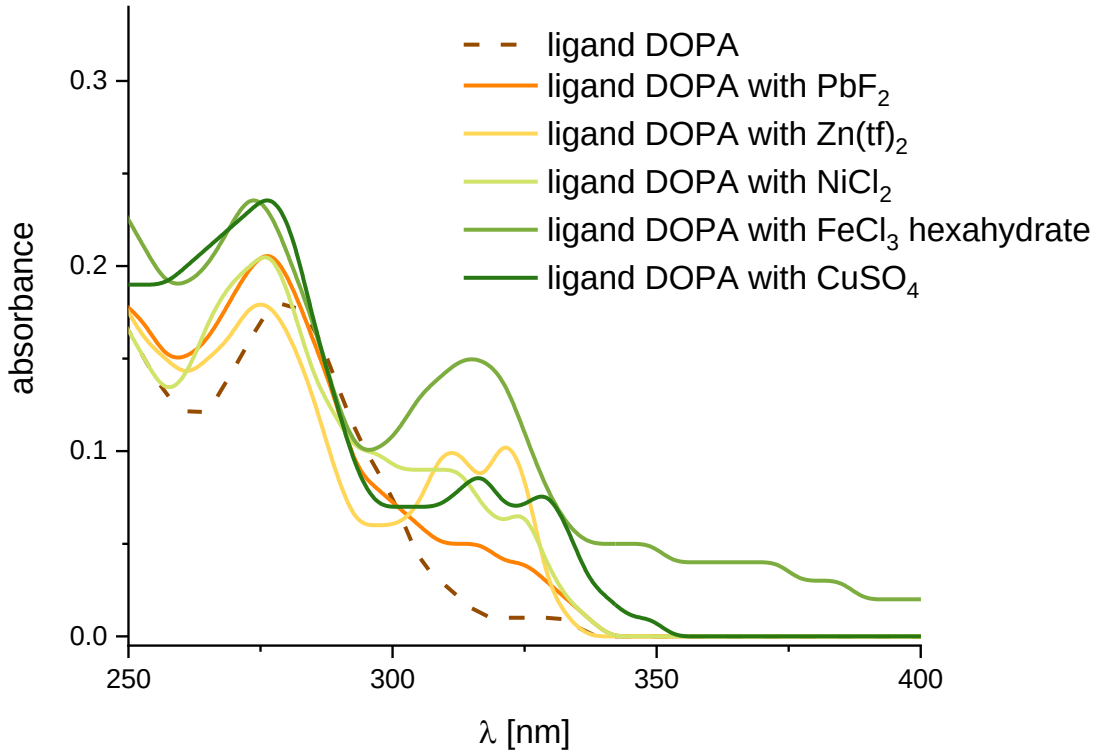

Figure S20. UV/Vis spectra of the DOPA containing the ligand, its complexes with PbF_2, $FeCl_3 \cdot H_2O$, $CuSO_4$, $Zn(tf)_2$ and $NiCl_2$, in $CHCl_3$/MeOH, concentration 2.6×10^{-5} mol L^{-1}.

7 Surface Coating

Surface Modification: Following a literature procedure[1], and since L-DOPA reacts immediately in presence of tris-buffer, two solutions were consecutively drop-casted. Initially, the Si wafers (1×1 cm^2) were placed into a petri dish, and 60 µL of a tris-buffer solution (0.3 M) was drop-casted onto the Si wafer. Subsequently, L-DOPA-containing moieties (2.7 mg dissolved in 60 µL EtOH) were drop-casted onto the Si wafer. The surfaces were subsequently left to react overnight, washed with Milli-Q water, and subsequently dried using a stream of N_2. Followed by analysis using XPS.

Fiber Coating with DOPA-modified Moieties: A Rockwool stone wool fiber cube measuring 1.5×1.5×0.5 cm^3 was dipped-coated in a solution containing a 1:1 ratio of tris buffer and L-DOPA-containing moieties for an overnight period. Following this, the fiber cubes were thoroughly washed using Milli-Q water and subjected to analysis using XPS and ToF-SIMS.

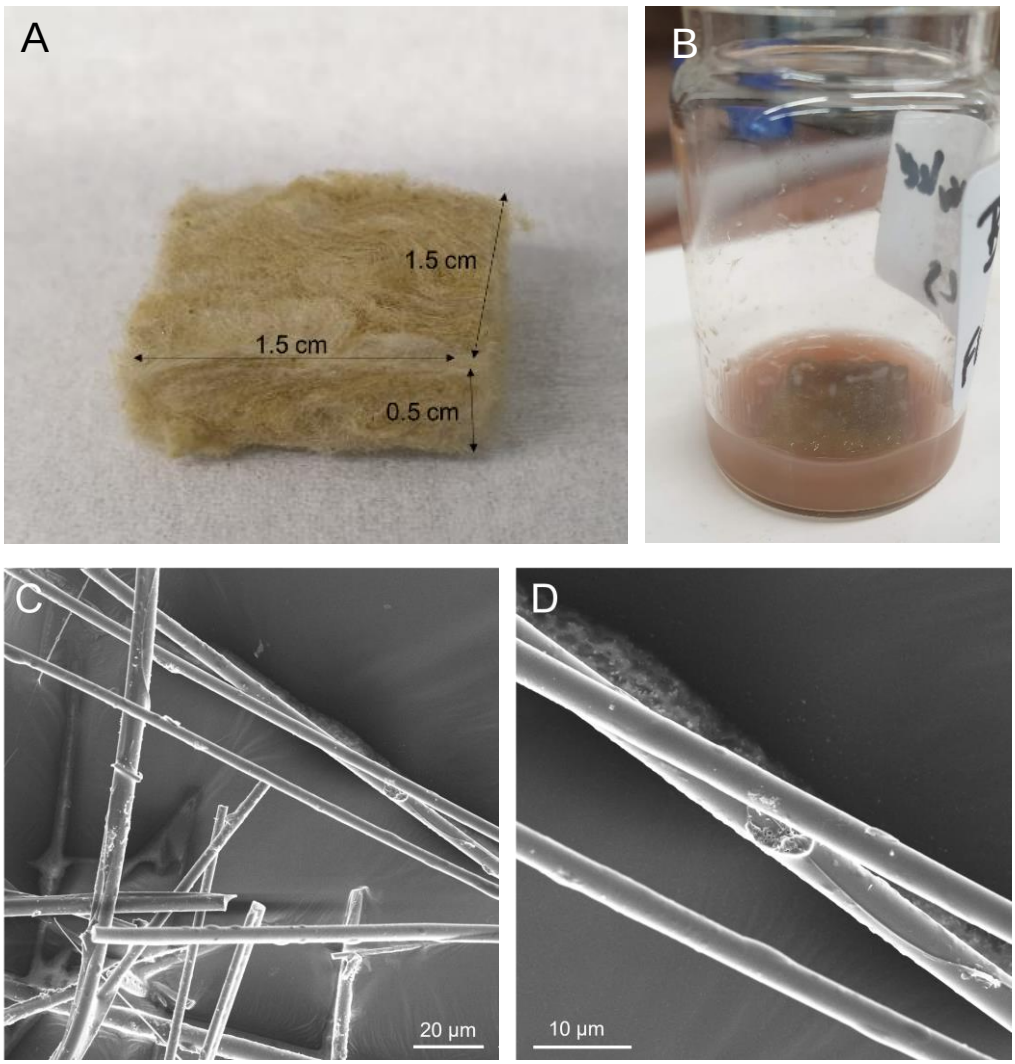

Figure S21. (A) Photo of a stone wool block cut into a small rectangle (1.5×1.5×0.5 cm^3) used for the fiber coating experiments and (B) set-up used for the fiber coating. The coating solutions were prepared in a snap cap vial and a stone wool piece was subsequently added. (C) and (D) represent SEM image of the coated fibres. The fibres have been observed to exhibit a range of diameters, ranging from 1 to 5 µm.

Metal Coordination on the Si Surfaces: Si surfaces coated with the ligand-modified L-DOPA were immerged in the metal solution (0.001 mol L^{-1}) for 30 minutes. Subsequently, the Si surfaces were thoroughly washed using Milli-Q water and subsequently dried using a stream of nitrogen, followed by XPS analysis.

Metal Coordination on the Fibres: Fibres coated with ligand-modified DOPA were immerged in the metal solution (0.001 mol L^{-1}) for 30 minutes. Subsequently, the fiber cubes were thoroughly washed using Milli-Q water and subjected to analysis using XPS and ToF-SIMS.

EDTA Experiments: After the silicon surfaces were coordinated to the metal according to the above section "Metal Coordination on Si Surfaces", the surfaces were immersed into an EDTA solution (2 mmol, pH=10) for 1 min, 10 min and 30 min, respectively. Subsequently, the surfaces were thoroughly washed using Milli-Q water and dried using a stream of N_2, followed by XPS analysis.

8 AFM measurements

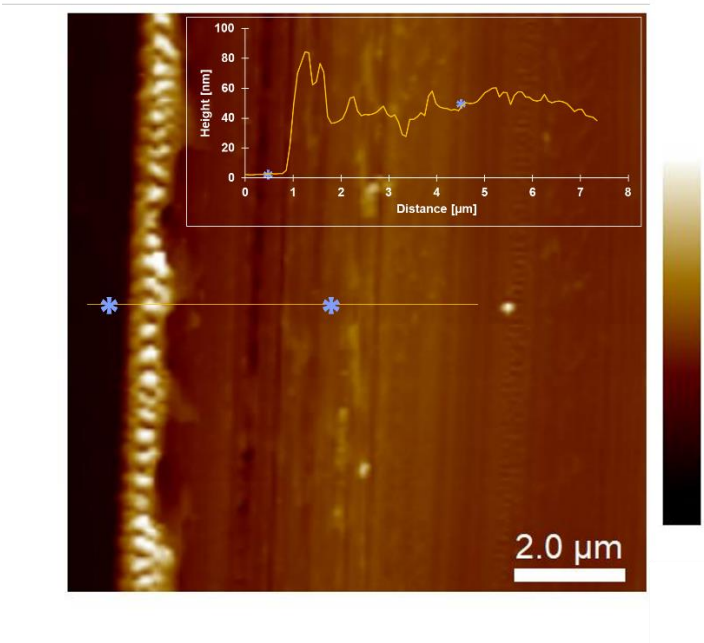

Figure S22. AFM image and the height profile (inset) showing the thickness of the ligand modified DOPA coating on an Si surface. The measured thickness of the coating is close to 40.6±1.1 nm.

9 XPS measurements

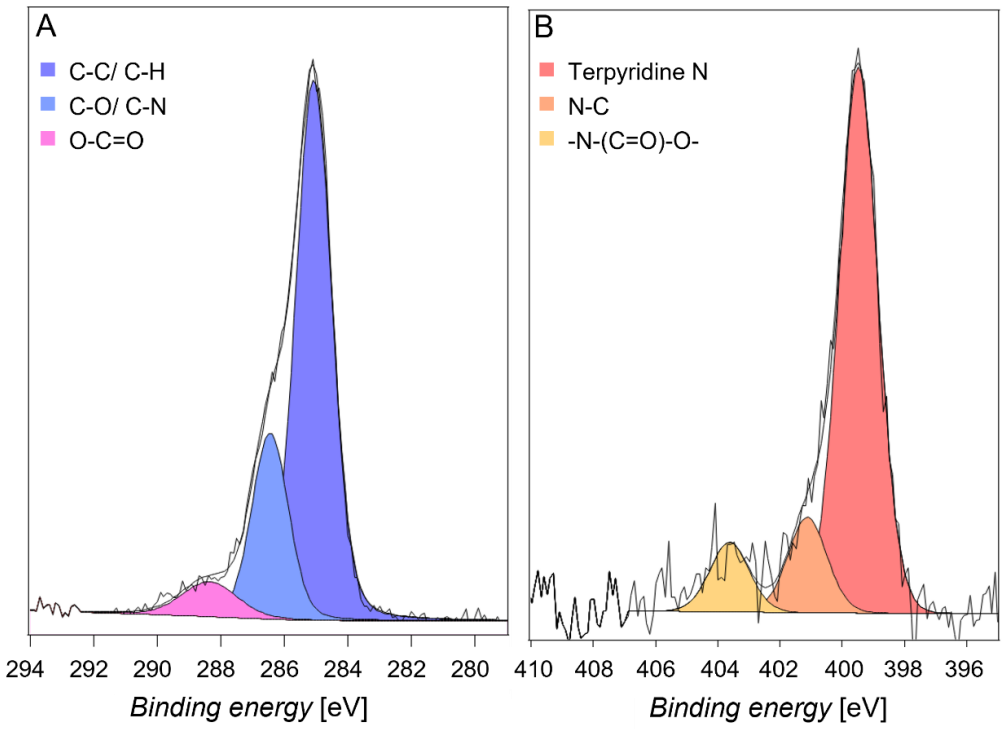

Figure S23. XPS high resolution spectra of (A) C 1s and (B) N 1s of terpyridine carrying L-DOPA on Si surfaces. C 1s is constituted of three main components associated with C-C/C-H at 285.0 eV, C-O and C-N at 286.3 eV, O=C-O at 288.3 eV. N 1s reveals three components associated with terpyridine N at 399.4 eV, N-C at 401.1 eV (possibly associated with dissociated BOC groups) and N-(C=O)-O- at 403.0 eV from the BOC group. The ratio between terpyridine N:(N-C + N-(C=O)-O-) = 1: 0.31, which aligns with the ligand modified DOPA.

We conducted additional investigations into the binding capabilities of ligand-modified L-DOPA (**7**) with other metal ions (Ni, Pb, Fe, and Cu) when applied as coatings on Si wafers. The procedures for coating the Si surfaces, preparing solutions containing the respective metal ions, and carrying out subsequent surface immersion steps were meticulously followed as detailed in Supporting Information Section 7. Figure S24 shows the XPS wide scan spectra of terpyridine functional surface exposed to (A) Cu^{2+}, (C) Ni^{2+}, (E) Fe^{3+}, and (G) Pb^{2+} with respective ligand-free L-DOPA control exposed to (B) Cu^{2+}, (D) Ni^{2+}, (F) Fe^{3+}, and (H) Pb^{2+}.

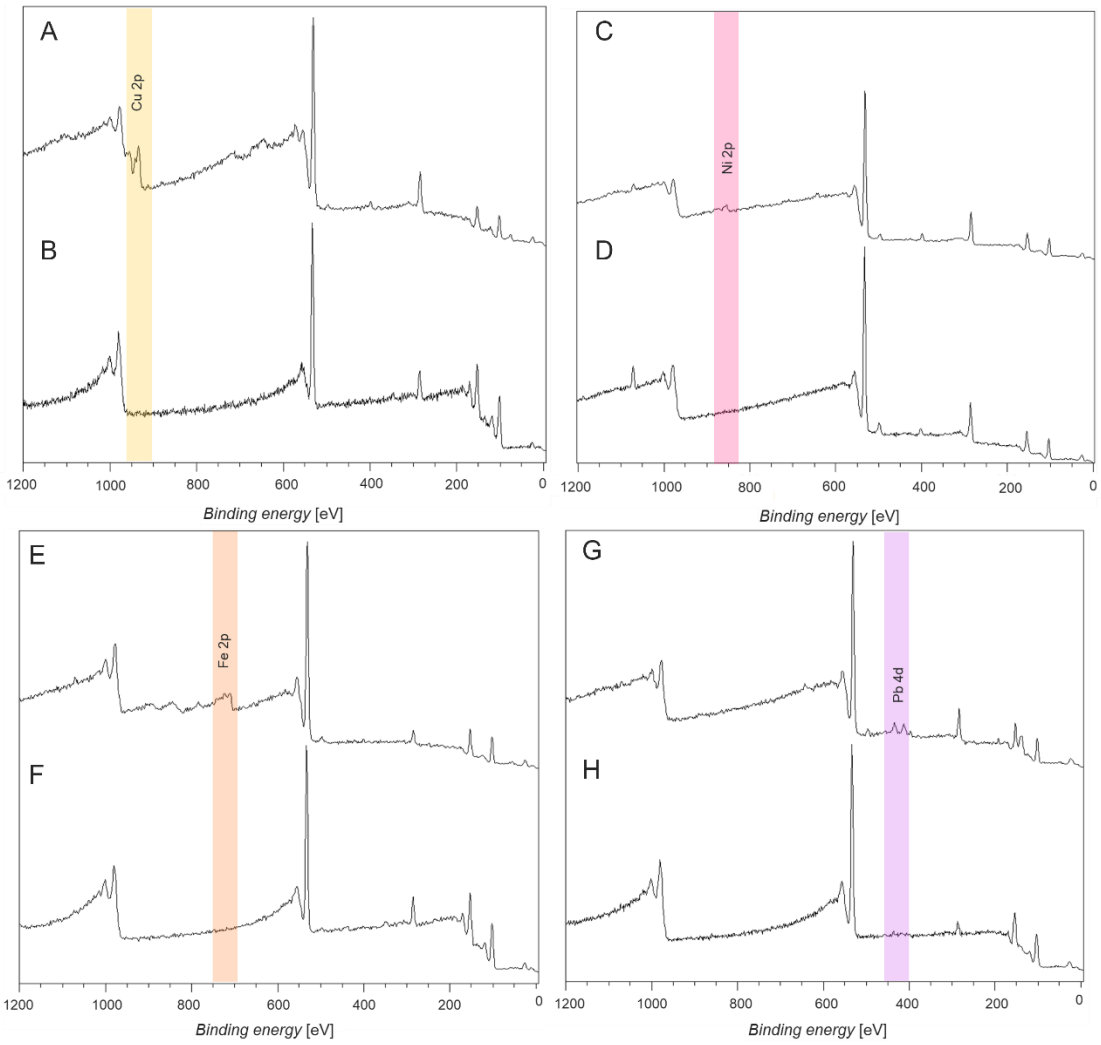

Figure S24. XPS wide scan spectra of Si-surfaces coated with ligand-modified L-DOPA, (A) and ligand-free L-DOPA (B) exposed to Cu^{2+}, Si-surfaces coated with ligand-modified L-DOPA (C) and ligand-free L-DOPA (D) exposed to Ni^{2+}, Si-surfaces coated with ligand-modified L-DOPA (E) and ligand-free L-DOPA (F) exposed to Fe^{3+}, and Si-surfaces coated with ligand-modified L-DOPA (G) and ligand-free L-DOPA (H) exposed to Pb^{2+}.

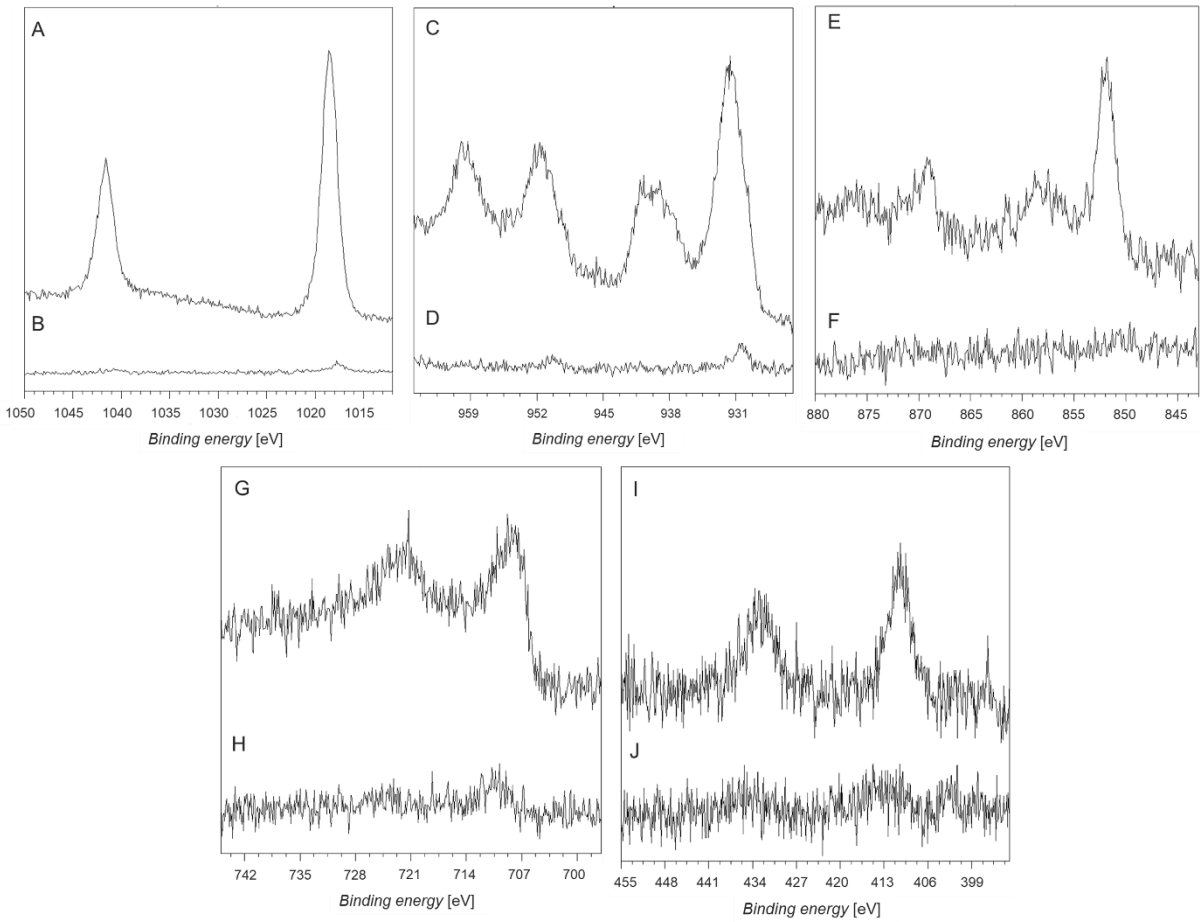

Figure S25. (A) XPS high resolution spectra of Si-surfaces coated with ligand-modified L-DOPA and ligand-free L-DOPA (B) exposed to Zn^{2+}, Si-surfaces coated with ligand-modified L-DOPA (C) and ligand-free L-DOPA (D) exposed to Cu^{2+}, Si-surfaces coated with ligand-modified L-DOPA (E) and ligand-free L-DOPA (F) exposed to Ni^{2+}, Si-surfaces coated with ligand-modified L-DOPA (G) and ligand-free L-DOPA (H) exposed to Fe^{3+}, and Si-surfaces coated with ligand-modified L-DOPA (I) and ligand-free L-DOPA (J) exposed to Pb^{2+}.

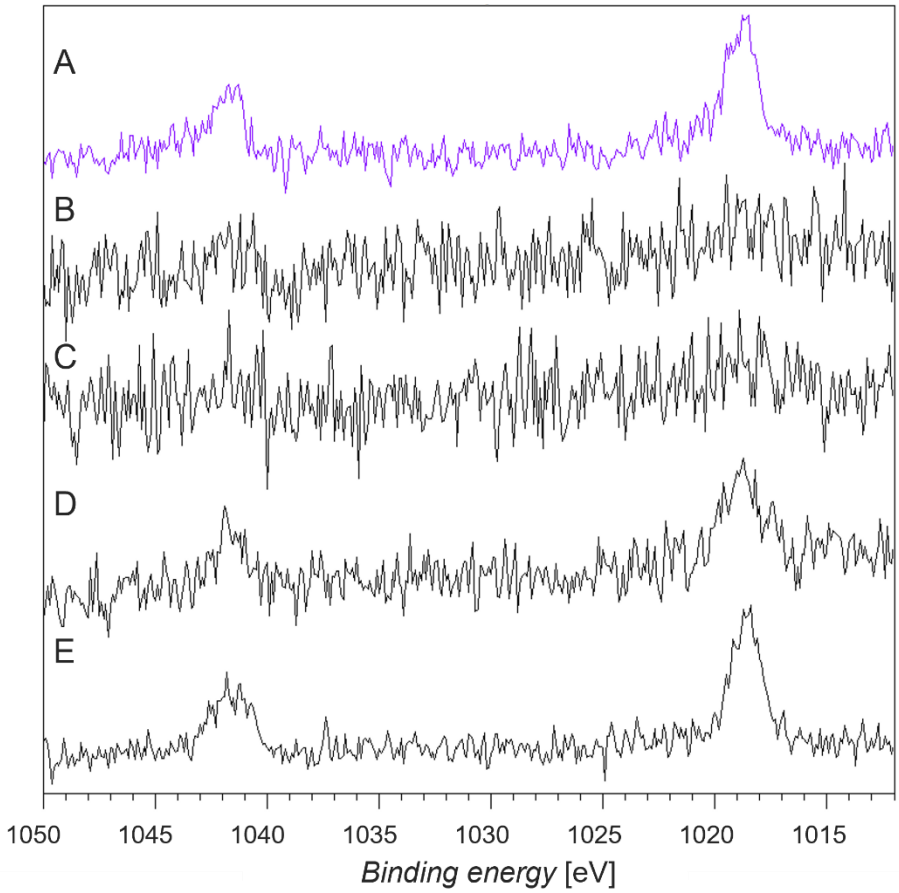

Figure S26. High resolution XPS spectra of Zn 2p (A) re-coordination of Zn^{2+} to the ligand-modified L-DOPA coated Si surface, which was previously exposed to EDTA for 10 minutes, (B) Zn^{2+} coordinated surface exposed to EDTA for 30 min, (C) Zn^{2+} coordinated surface exposed to EDTA for 10 min, (D) Zn^{2+} coordinated surface exposed to EDTA for 1 min, and (E) initial Zn^{2+} coordinated to ligand-modified L-DOPA coated Si surface.

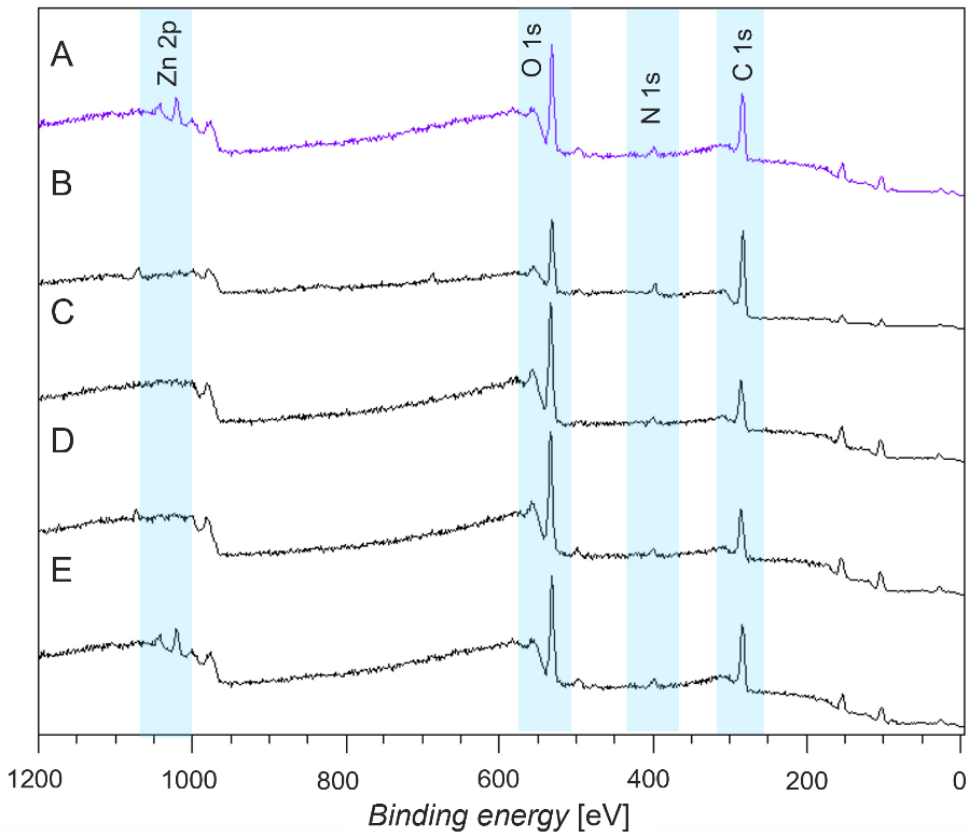

Figure S27. Wide XPS spectra of Zn 2p (A) re-coordination of Zn^{2+} to the ligand-modified L-DOPA coated Si surface, which was previously exposed to EDTA for 10 minutes, (B) Zn^{2+} coordinated surface exposed to EDTA for 30 min, (C) Zn^{2+} coordinated surface exposed to EDTA for 10 min, (D) Zn^{2+} coordinated surface exposed to EDTA for 1 min, and (E) initial Zn^{2+} coordinated to ligand-modified L-DOPA coated Si surface.

To investigate the removal of the metal from the terpyridine carrying L-DOPA, we calculated the ratio of Zn^{2+} to Si after each varying exposure times to EDTA, by comparing the area under the curve of the Zn 2p and Si 2p peaks, determining the relative amounts of Zn present on the surface.

Table S1. Analysis by XPS region to determine the Zn to Si ratio.

Sample	Zn 2p	Si 2p	Zn/Si%
Zn coordinated	4.21	95.78	0.44±0.14
Exposure time to EDTA, 1 min	0.61	99.38	0.06±0.05
Exposure time to EDTA, 10 min	0	97.55	0
Exposure time to EDTA, 30 min	0	98.61	0
Zn re-coordinated	3.89	96.17	0.39±0.13

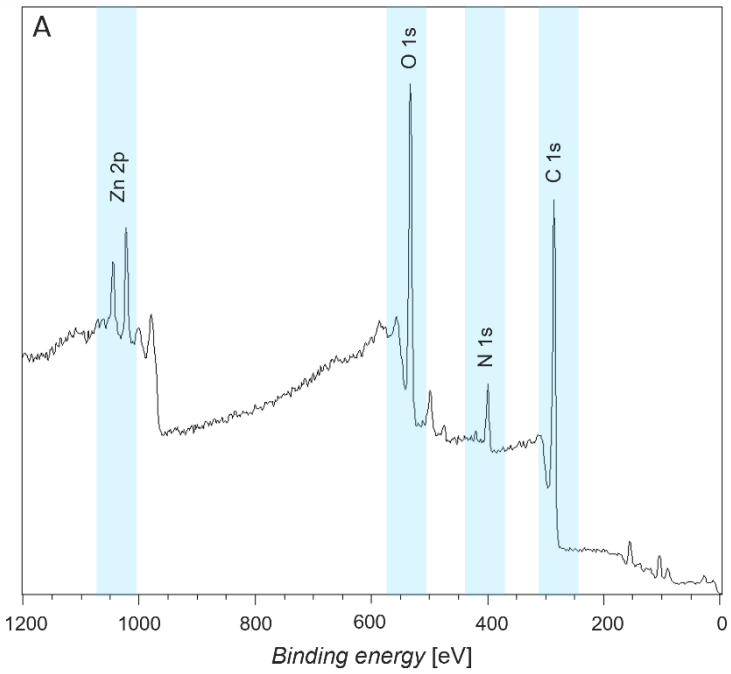

Figure S28. XPS wide scan spectra of control experiments to determine the effect of pH on the efficacy of metal removal. (A) shows the Zn^{2+} coordinated terpyridine carrying L-DOPA substrate exposed to pH =10 in solution for 10 min. After 10 min, the metal ion is still coordinated to the ligand, evidencing that pH has no effect on the ability of EDTA to remove the metal from the surface.

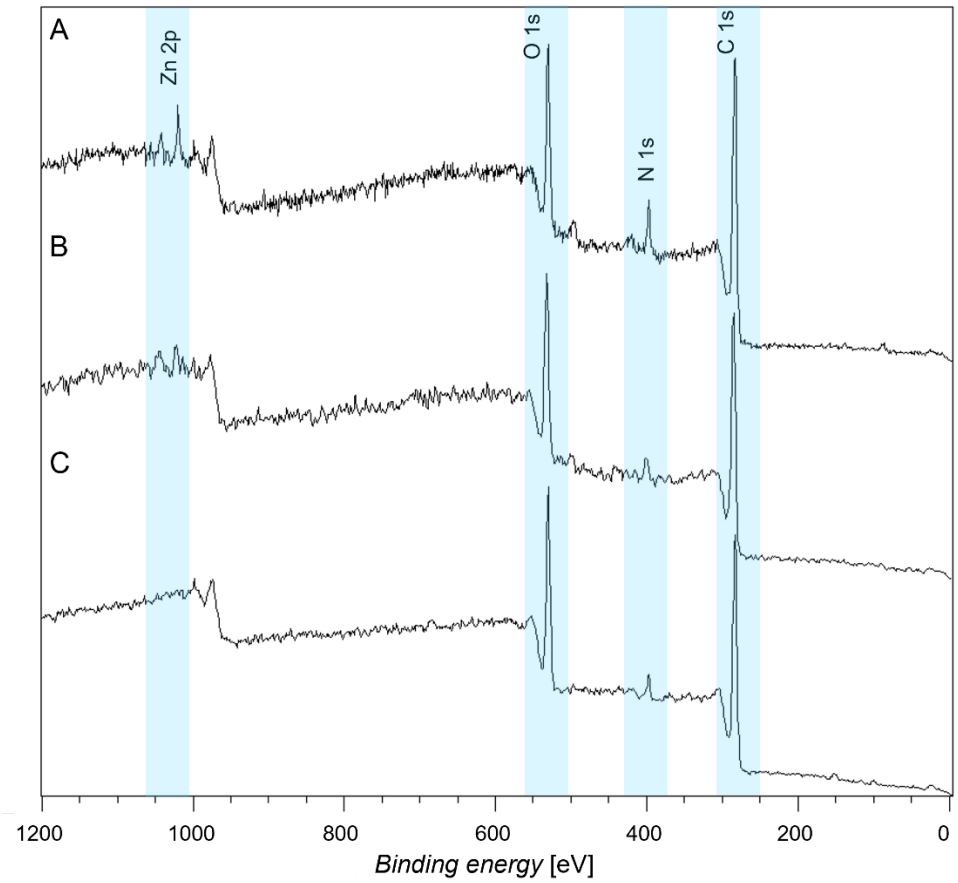

Figure S29. Comparison XPS wide spectra of (A) fibres coated with ligand-modified L-DOPA (**7**), exposed to Zn^{2+} solution; (B) fibres coated with ligand free L-DOPA exposed to Zn^{2+} solution, and (C) pristine fibres exposed to Zn^{2+} solution.

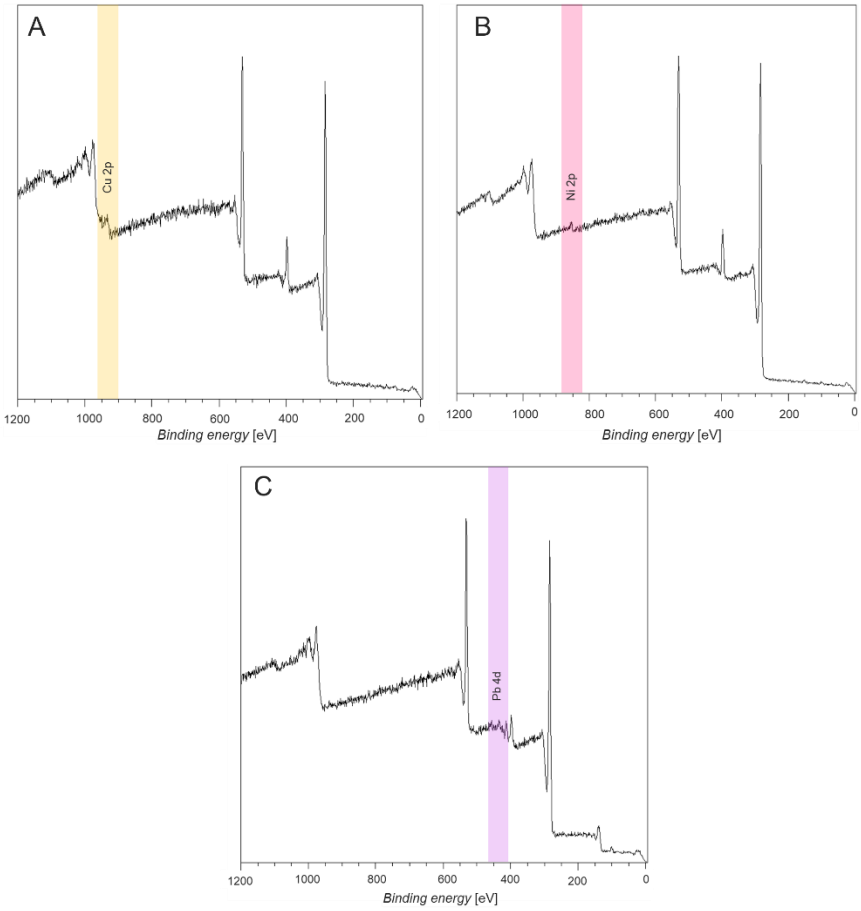

Figure S30. Additional experiments were carried out to investigate the ligand-modified L-DOPA coated fibres ability to coordinate other metals**.** XPS wide spectra of fibres coated ligand-modified L-DOPA, (A) exposed to Cu^{2+} solution, (B) Ni^{2+} solution, and (C) Pb^{2+} solution.

10 ToF-SIMS measurements

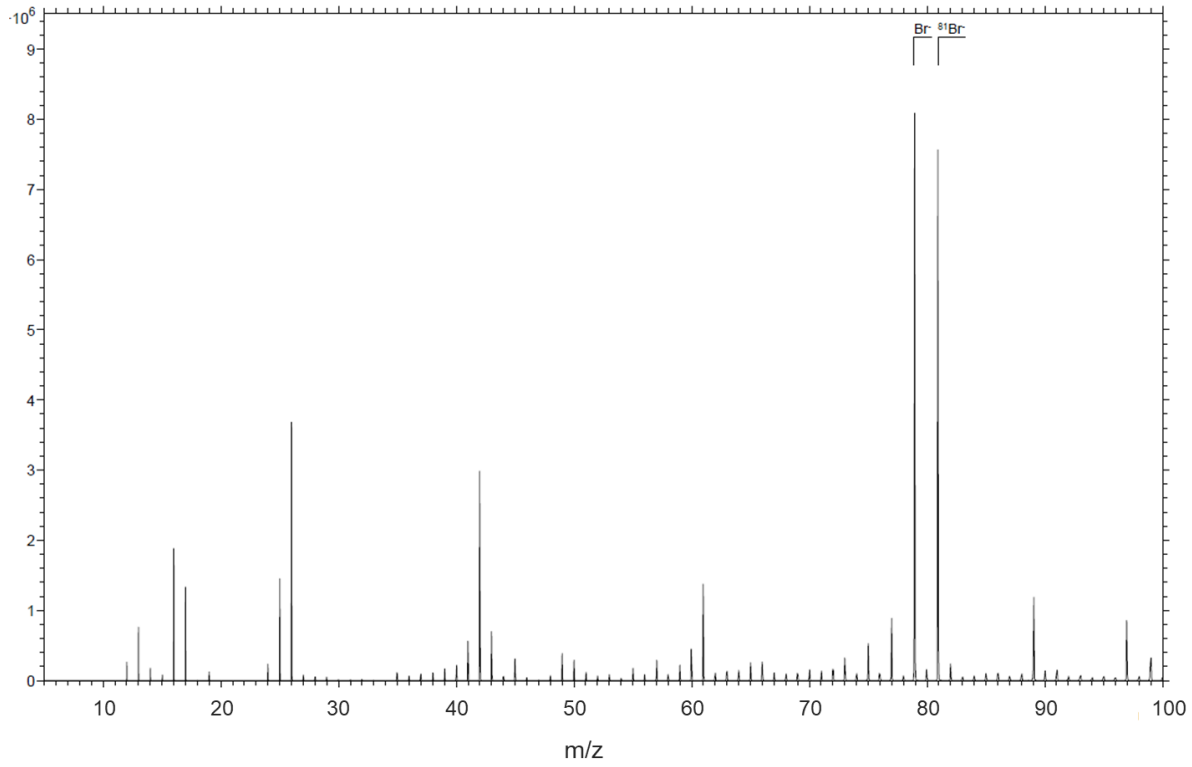

Figure S31. ToF-SIMS spectra of silicon surfaces coated with Br-modified L-DOPA.

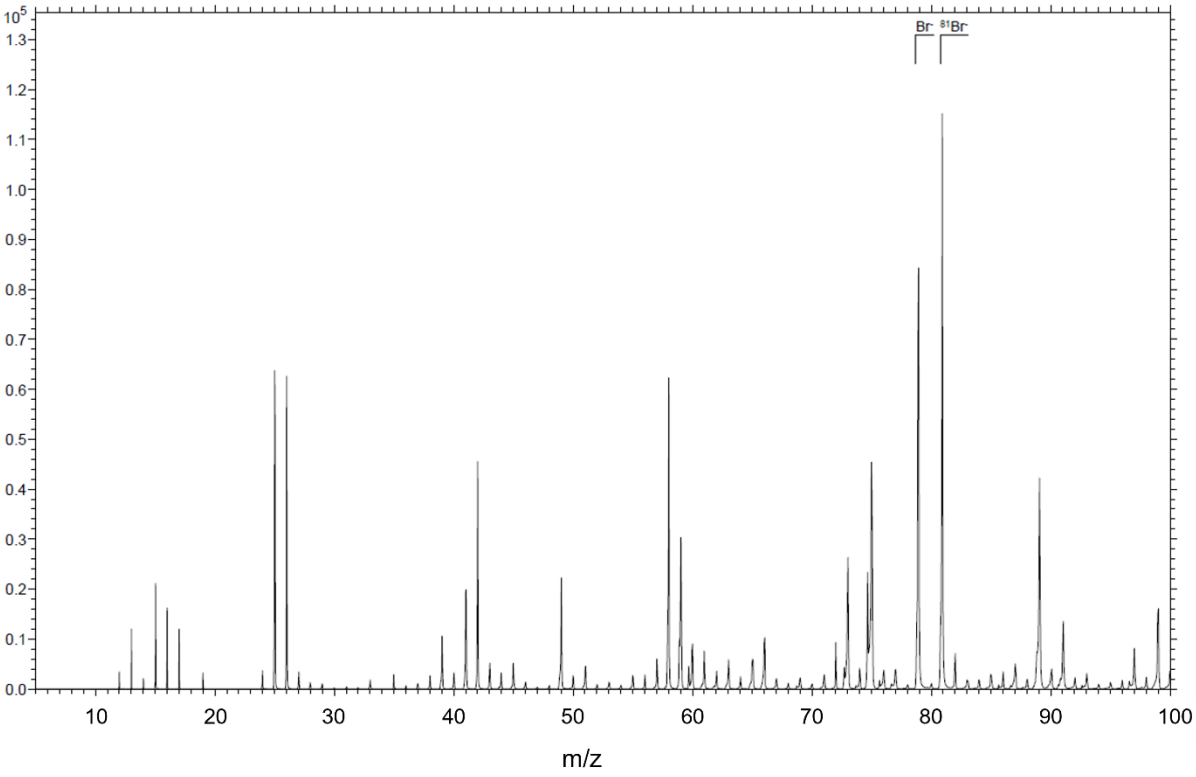

Figure S32. ToF-SIMS spectra of fibres coated with Br-modified L-DOPA.

11 XPS investigations on mixed metal solutions

Additionally, we investigated the affinity of the different metals in mixed metal solutions. Similar to the XPS measurements that were conducted with a single metal solution, Si surfaces were coated with ligand-modified L-DOPA. The coated surfaces were then immersed in metal solutions containing zinc and another metal for 30 minutes and subsequently analysed by XPS. The preparation of the metal solutions (Zn^{2+}, Ni^{2+}, Pb^{2+}, Fe^{3+}, and Cu^{2+}) and the immersion procedure were conducted in Section 7 of the Supporting Information section.

Figure S33 depicts the XPS-wide scan of the different combinations of the two metal solutions tested on the Si surfaces coated with ligand-modified L-DOPA. Quantitative XPS analysis was conducted to assess the ratio of metal ion coordination to ligand-modified L-DOPA on the silicon surface. **Figure S33A** reveals that in a mixture of Zn and Pb metal ions a ratio of 0.5:1.0 (Zn: Pb) is present. A ratio of 0.1:0.3 (Zn: Fe) can be found for the Zn/Fe mixture (**Figure S33B**). The experiment featured in **Figure S33C** revealed no presence of Zn ions ion the surface in a Zn/Cu mixed solution. Similarly, **Figure S33D** shows no presence of Ni on the surface in a Zn/Ni mixed solution. Finally, **Figure S33E** indicates that when combining Pb and Fe there is no detection of Pb on the surface, solely Fe.

In summary the results indicate that that the metal coordination affinity progresses from $Fe^{3+} > Pb^{2+} > Cu^{2+} > Zn^{2+} > Ni^{2+}$. The observed trend in metal-ion coordination aligns with results for metal binding in solution.[3]

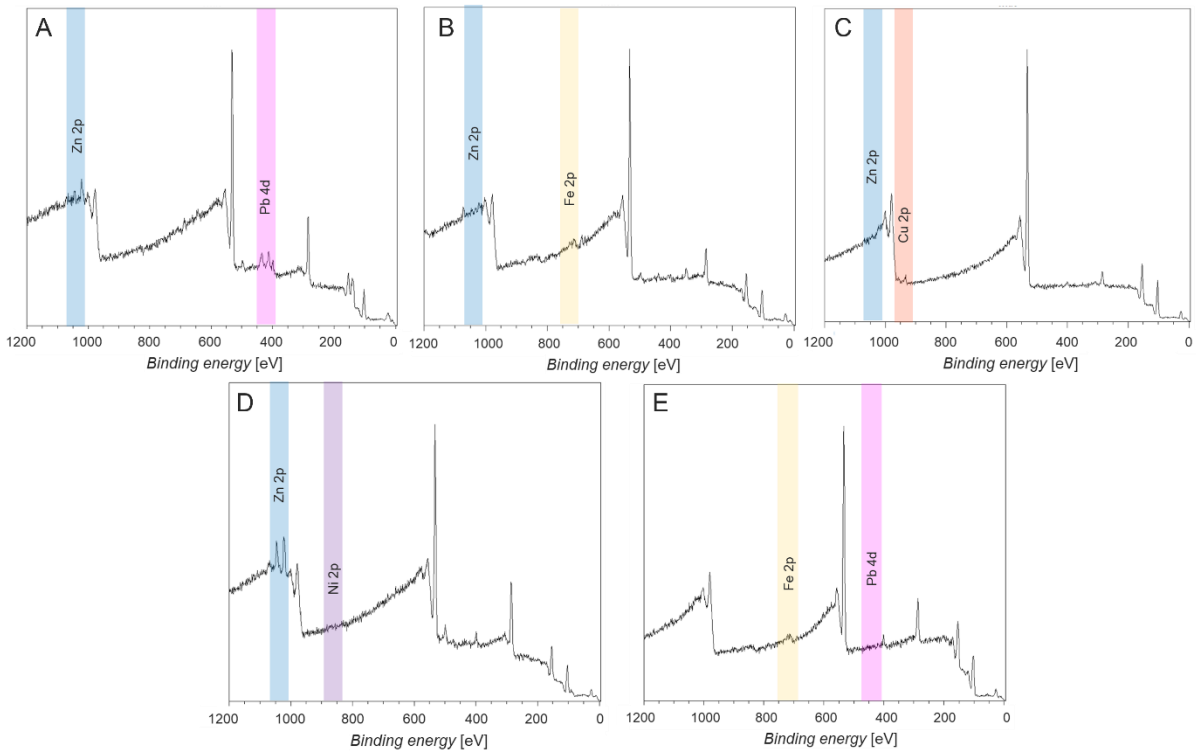

Figure S33. XPS wide scan spectra of metal mixtures coordinated to the ligand-modified L-DOPA on Si surfaces, (A) Zn and Pb, (B) Zn and Fe (C) Zn and Cu (D) Zn and Ni, (D) Fe and Pb (E).

12 References

1. C. M. Preuss, T. Tischer, C. Rodriguez-Emmenegger, M. M. Zieger, M. Bruns, A. S. Goldmann and C. Barner-Kowollik, *J. Mater. Chem. B.*, 2014, **2**, 36-40.
2. S. Bode, L. Zedler, F. H. Schacher, B. Dietzek, M. Schmitt, J. Popp, M. D. Hager and U. S. Schubert, *Adv. Mater.*, 2013, **25**, 1634-1638.
3. H. A. Saadeh, E. A. A. Shairah, N. Charef and M. S. Mubarak, *J. Appl. Polym. Sci.*, 2012, **124**, 2717-2724.